CLIMATE TRADE COSTS

Hubert Massoni*

Preliminary and Incomplete: Latest Version

ABSTRACT

This paper examines the impact of extreme weather events on global supply chains through disruptions to trade infrastructure in a context of climate change. Leveraging high-frequency administrative data covering the quasi-universe of firm-to-firm maritime shipments from the US and Brazil, I study the impact of tropical cyclones on US port operations and firm-level responses. These weather events temporarily disrupt port activities, prompting firms to reduce trade volumes without significantly terminating relationships. Firms however demonstrate persistent adjustments in route choices, even after ports resume normal operations. To evaluate the general equilibrium implications of these transportation-related weather disruptions, I develop a quantitative model of spatial production networks with endogenous trade costs and traffic congestion. Once taken to the data, the model will serve to quantify spatial reallocation of economic activity induced by increasing climate risks to the transportation network, and the effectiveness of port-level infrastructure policy.

*University of Bologna. Email: hubert.massoni2@unibo.it. I am particularly grateful to Emanuele Campiglio and Bruno Conte for their excellent guidance and support. This paper benefited from conversations with Clare Balboni, Johannes Boehm, Mathieu Couttenier, Pierre Coster, Alejandro Graziano, Vasily Korovkin, Isabelle Méjean, David Nagy, Giacomo Oppocher, Filippo Pavanello, Lavinia Piemontese, Filippo Santi, Vincenzo Scrutinio, Alessandro Sforza, Edouard Schaal, Tommaso Sonno, Jaume Ventura, and from the comments of numerous seminar and conference participants. I am grateful to Alireza Naghavi for kindly sharing data.

1 Introduction

Transportation infrastructure is the backbone of international trade and channels large investments to improve efficiency and resilience. Yet, disruptions related to transportation and logistics are common and expose firms to bottlenecks, delays, and uncertainty in shipping (Blaum et al., 2024). Transportation infrastructure is particularly vulnerable to extreme weather events. The case of maritime ports, located at low altitudes in riverine areas and therefore prone to storm surge, high wind speeds, and floods, is a prime example of such vulnerability. Weather-related hazards put not only the physical infrastructure of ports at risk but also the trade flows that rely on it (Verschuur et al., 2023b).[1] Firms' responses to port downtime, particularly re-routing, can amplify these disruptions through congestion in alternative itineraries (Allen and Arkolakis, 2022; Brancaccio et al., 2024). The advent of climate change, likely to increase the frequency and intensity of extreme weather events, raises the question of whether firms' responses to weather-related transportation disruptions can mitigate global supply chain exposure to shipping uncertainties.

I explore two potential responses of firms to transportation-related weather disruptions: (i) supply chain re-composition — adjusting the set of exposed suppliers — and (ii) re-routing — diverting away from risky infrastructure. Capturing these adaptation margins and their impacts on the economy poses several challenges. First, one needs detailed information on firm-to-firm linkages and the transportation infrastructure they rely on. Second, to quantify the general equilibrium impacts of such transportation disruptions, one needs a theory of firm linkage formation at a fine spatial granularity that accounts for complex routing decisions and the congestion spillovers they might imply on the transportation network.

I address these challenges by leveraging high-frequency administrative data of international maritime trade at the shipment level. The data contain information on the nature of shipments, on each trading firm, and on the port infrastructure used to ship the goods. Merging the trade data with detailed information on tropical cyclones' trajectories and characteristics, I study the effect of US maritime ports' exposure to high-speed winds and the responses of Brazilian firms. I also develop a quantitative model of spatial production networks with endogenous transportation costs and traffic congestion. Once calibrated, the model can quantify how transport-related weather disruptions induced by climate change translate into increased traffic congestion, supply chain recompositions, and welfare losses.[2]

Studying the context of US ports exposed to tropical cyclones and the responses of

[1] Studying 1,340 ports globally, Verschuur et al. (2023b) find that 86% of ports are exposed to more than three weather-related hazards. Port-specific risk totals 7 billion USD per year, with 32% of the risk attributed to tropical cyclone impacts, while 63 billion USD of trade is at risk every year.

[2] Quantitative calibration and results are not yet included in the paper.

Brazilian firms provides me with an ideal setting to infer firm-level adaptation margins induced by transportation-related weather disruptions. First, maritime ports are key infrastructure of international trade, responsible for more than 80% of global trade volumes. Port disruptions can temporarily reduce the freight volume ports can process, causing delays, depreciation of goods, and, in cases where cargo is re-routed, additional transportation costs. Second, maritime ports are particularly vulnerable to weather disasters, being located along coastlines and river shores.[3] Tropical cyclones are among the most prevalent sources of risk, inducing high-speed winds, heavy rainfall, and floods (Verschuur et al., 2020). Although the tropical storms affecting the US are concentrated within a well-defined storm season (June 1 to November 30), the location, timing, and intensity of the events remain largely unpredictable (Hsiang and Jina, 2014). Third, the exposure of US-to-Brazil trade flows to these disruptions is large. US exports of goods to Brazil amount to more than 50 billion USD per year.[4] Brazilian ports, however, are rarely affected by tropical cyclones.[5]

Using recent advancements in the difference-in-difference literature (Dube et al., 2023), I provide empirical evidence that port exposure to tropical cyclones affects firm-to-firm trade and prompts persistent firm responses along routing decisions. I first show that tropical cyclones temporarily disrupt the operations of US maritime ports, for an average duration of four days around the cyclone's landfall.[6] Second, I document that these disruptions induce a three-month decrease in firm-to-firm activity. Firms delay or cancel shipments for a quarter before resuming linkage activity. The cyclone events are not disruptive enough to break relationships, as I do not observe a significant increase in the probability of relationship termination. Third, I show that the adaptation margin of firms lies in the routing decision. Firms permanently re-route trade away from the affected ports: the probability of using an exposed route declines by 45% up to one year after the event. Given that the ports quickly resume operations, I interpret these results as adaptation responses to the occurrence of an extreme weather event.

To address further challenges related to quantifying the economic impact of these disruptions in a context of climate change, I build a model of spatial production networks with endogenous trade costs affected by weather disruptions. The model accounts for traffic congestion, which likely induces economic agents to re-optimize

[3] A survey conducted by UNCTAD (2018) suggested that 72% of the responding port authorities have been impacted by extreme weather events, causing delays (60%), disruption of operations (76%), or physical damages (45%).

[4] The US is the second import partner of Brazil. Brazil is the 11th export partner of the US.

[5] Brazil's coastal regions lie near the equator, where temperature variations are minimal and winds primarily move vertically. Due to the weak convergence zone of trade winds in this area, tropical cyclones do not form.

[6] Because port authorities forecast the cyclones' trajectory and intensity, port downtime can anticipate the landfall. I use precautionary thresholds of the US Coast Guards to inform my definition of a port-level shock (condition ZULU). See Section 3.1.

routing. The empirical evidence I provide demonstrates that firms re-route trade toward safer routes following weather disruptions. However, if traffic congestion raises the costs of using these alternative routes, such routing responses could impact other parts of the transportation network. Furthermore, while I empirically capture firm responses to individual weather events, I cannot address a broader shift in the distribution of such events — an essential feature of climate change.[7] The model allows for such a counterfactual scenario by assuming that a shift in firms' perfectly informed beliefs about the likelihood of weather disasters mirrors a sequence of realized events. Through this process, firms continually update their information about the probability of extreme weather events, enabling an analysis of long-term adaptation dynamics.

In the model, firms located across cities require intermediate inputs to produce final goods. They take a joint sourcing and routing decision over the beliefs they form on factory-gate costs and transportation costs, to find the most cost-effective supplier and delivery route for the inputs. Road transportation is allowed when cities are directly connected through land, and maritime transportation when both cities contain port infrastructure. Shipping through port infrastructure entails additional weather-related costs, drawn from a distribution which is perfectly known by economic agents. Transportation costs are endogenous to traffic, and inversely related to infrastructure capacity.

I structurally estimate the components of transportation trade costs using the Brazilian microdata, and confirm three predictions of the model: (i) port-level traffic leads to congestion, and results in an increase in transportation costs, (ii) these congestions are alleviated by port capacity, (iii) transportation costs are affected by wind conditions around ports. A 1% increase in yearly expected windspeed at the port level increases transportation costs by 0.02% — close to 25% of the effect of port congestion.

I calibrate the model at the sub-national level (GAUL1), and use the tropical cyclones probabilistic set projections of the STORM model to infer the climate-change-induced increase in extreme wind events at the port level. The model can quantify the distributional impacts of a shift in the distribution of extreme-weather events on maritime ports. An increase in the probability of extreme weather events unambiguously increases transportation costs of routes that use the affected ports. Traffic congestion, on the other hand, creates negative spillovers to nearby ports. To explore further adaptation mechanisms, which do not relate to private firms' responses already embedded in the model, I propose another counterfactual scenario in which a social planner can reallocate port capacity across the country's existing port infrastructure. As traffic congestion is inversely related to the capacity of infrastructure, decreasing the capacity of

[7] Although the intensity and frequency of tropical cyclones affecting US shores have increased since the 2000s (see Appendix A.1), the link with climate change is arguably unclear (Vecchi et al., 2021). Besides, the data I use on maritime shipments only covers six years, and therefore does not allow for observing the effect of such a distributional shift.

ports that are most affected by weather disruptions increases incentives to use alternative routes, less likely to experience weather disruptions. *(This section is in progress, and not included in the present version of the paper.)*

Related Literature. This study is first and foremost related to the growing literature assessing the impact of natural disasters and extreme weather events on production networks (Barrot and Sauvagnat, 2016; Boehm et al., 2019; Carvalho et al., 2021). Both the empirical and theoretical exercises of this paper are most closely related to the recent works of Balboni et al. (2024) and Castro-Vincenzi et al. (2024), documenting the impact of floods on domestic supply chains, and the adaptive responses of firms. Their findings that firms form and update beliefs on the underlying distribution of weather-related disruptions following the occurrence of an event constitute the stepping stones on which I read my empirical results. A key difference to my setting is that they primarily study the impact of floods on firm premises. I focus on a complementary mechanism related to transport-related disruptions, the role of traffic congestion in inducing further negative spillovers, and of mitigating infrastructure policy.[8]

Second, this paper is related to the literature considering the role transportation costs and infrastructure play in shaping economic activity. A subset of the literature explores the endogeneity of transportation costs to traffic congestion (Brancaccio et al., 2020; Fajgelbaum and Schaal, 2020; Allen and Arkolakis, 2022). I draw from the framework of Allen and Arkolakis (2022) and incorporate in the model an optimal transportation problem defined as firms selecting bilateral least-cost routes.[9] I extend the transportation network to port infrastructure subject to capacity constraints that directly affect traffic congestion (Ducruet et al., 2024; Brancaccio et al., 2024). Another related branch of the literature focuses on the effects of transport-related delays and disruptions, and their consequences on firms' sourcing decisions (Volpe Martincus and Blyde, 2013; Martinez, 2024; Blaum et al., 2024; Clark et al., 2024). I complement their findings by studying a setting in which I can more precisely identify the trade infrastructure used to ship goods within firm-to-firm relationships.

Finally, this paper is related to a broader literature assessing the distributional impacts of climate change on economic activity (Bilal and Rossi-Hansberg, 2023; Desmet and Rossi-Hansberg, 2015; Cruz and Rossi-Hansberg, 2024; Rudik et al., 2021). A subset of this literature highlights the role of firms' decisions in shaping adaptation to

[8] Balboni et al. (2024) do consider flood-induced road disruptions and the subsequent responses of firms as part of their results, using detailed GPS tracker data from commercial trucks. The data do not, however, allow for observing the exact road infrastructure through which goods are shipped. Furthermore, the effects of weather disasters on transportation costs is not explicitly incorporated in their quantitative model.

[9] Subsequent works consider extensions of this framework to maritime trade with increasing returns to scale in traffic (Ganapati et al., 2024), and endogenous port size (Ducruet et al., 2024), or to multi-mode transportation networks (Wong and Fuchs, 2022).

climate risks.[10] These works put an emphasis on how firms adjust their set of suppliers, location of production, entry and exit, or investments following extreme weather events (Pankratz and Schiller, 2021; Castro-Vincenzi, 2024; Jia et al., 2022; Rabano and Rosas, 2024). I focus on an additional margin of adaptation related to re-routing, and suggest that firms' responses should be complemented with infrastructure policy to account for negative congestion spillovers.

The rest of the paper proceeds as follows. Section 2 describes the data. Section 3 provides empirical evidence on firms' responses to transportation-related weather disruptions. Section 4 incorporates these responses into a theoretical model of production network formation with traffic congestion and weather-induced transportation costs. Section 5 discusses the model parametrization and calibration. Section 6 provides insights on the future quantitative exercises I will conduct. Section 7 concludes.

2 Data

In this section, I describe the data I use in the empirical Section 3. The main sources of data that allow me to study firm-to-firm relationships and port-level outcomes are bill of lading data from the US and Brazil. A bill of lading is a document issued by a carrier to acknowledge receipt or shipment of cargo. It usually contains information on the cargo's origin, destination, quantity, packaging, shipping details, and cargo description. I use the bill of lading data from Brazilian imports to recover relationship outcomes, as it contains the identifiers of both the origin and destination parties at the establishment level. The bill of lading data for US exports does not contain information on the destination establishment (the foreign buyer). I use it to recover port-level outcomes. I combine the bill of lading data with tropical cyclone tracks and climate data.

Firm-to-firm shipments. I study firm-to-firm relationships and trading routes using bill of lading data assembled by S&P Panjiva. The dataset encompasses the universe of maritime import transactions conducted by Brazilian firms between June 2014 and December 2019. Each shipment entry includes unique identifiers for both the Brazilian importer and the foreign exporter, based on parent company names. Geographic details, such as street address, city, postal code, and country, are recorded for each trading party, allowing precise geocoding of shipment origins and destinations. The data also track the maritime ports of origin and destination for each shipment, enabling the reconstruction of trading routes. Each transaction is classified by a 10-digit

[10] An extensive survey on firm adaptation to climate change is provided by Grover and Kahn (2024).

Harmonized System (HS10) code, providing detailed information on the nature of the traded product. The dataset records the weight, volume, and current US dollar value of each shipment. An indicator informs whether the shipment cargo is owned by the trading parties or whether they are forwarders of the goods — i.e., merely third parties transporting the goods.

I perform a series of steps to clean the data and restrict attention to trade between production-oriented, regularly trading, and geolocalized parties. I refer to geolocalized establishments belonging to an identified parent company as *firms*.[11] First, all shipments with missing parent company name or port ID are removed, since I cannot identify the trading parties or routes. Second, I obtain firm geolocalization through an ArcGIS geocoder and remove from the sample firms that are not geolocalized at the city or postal code level. Third, to avoid noise generated by infrequent relationships, I remove all pairs of firms trading only once. Fourth, I restrict attention to all shipments for which both parties are declared the real owners of the cargo, thereby removing warehouses or transportation companies from the sample. Fifth, I remove all importers not geolocalized in Brazil and all exporters geolocalized in Brazil.

Throughout the empirical section, I denote Brazilian importers as *buyers* (indexed by b), foreign exporters as *suppliers* (indexed by s), and buyer-supplier pairs $\{b, s\}$ as *relationships*. Based on the location of establishments, I assign to each supplier and buyer their location (or 'city' in Section 4) at the GAUL1 level, respectively denoted n_o for the origin location, and n_d for the destination location. When shipments transit from a port of origin p_o to a port of destination p_d, I denote the quadruplet $\{n_o, n_d, p_o, p_d\}$ as a *route* (indexed by r). The final sample contains 545,259 shipments, from 9,105 suppliers, to 7,853 buyers, through 1,088 routes. Appendix B.1 describes the sampling procedure and provides summary statistics on firm-to-firm trade. Figure 1a presents the geographic distribution of firms in the sample.

US port-level activity. To construct US port-level outcomes, I use US bill of lading data assembled by S&P Panjiva, which covers all maritime export transactions from US firms to foreign countries between January 2011 and December 2019.[12] The data contain information about the exporting parent company, geographic information on the shipment origin (the establishment), the port of origin through which the shipment leaves the US, and the name of the vessel carrying the goods. To recover the UN/LOCODE of the ports, I manually match the US port names in the Panjiva dataset

[11] To palliate frequent typos in company names and geographic details, I clean the name strings, and assign to a single firm ID all establishments belonging to a parent company name and geolocalized within a 10km radius.

[12] This dataset is the US counterpart of the Brazilian transaction data. I do not use it to run firm-level regressions, however, given that it does not contain information about the foreign buyer of shipments — only about the country of destination.

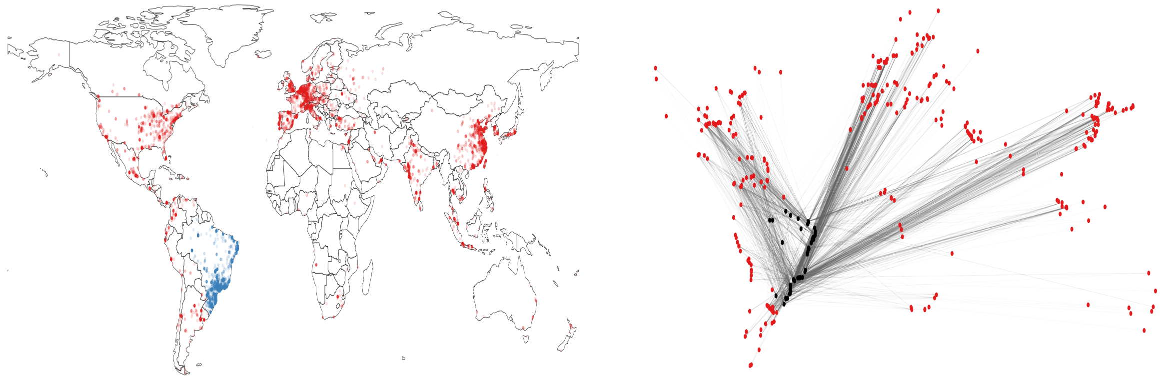

(a) Location of trading firms (b) Maritime routes

Notes: Panel 1a maps the location of the firms selected in the final sample. Each dot represents a firm: red dots are foreign suppliers (n=9,105), and blue dots are Brazilian buyers (n=7,853). Panel 1b maps the location of the ports, and the associated active routes within the sample. Each dot represents a port: red dots are foreign ports of exit (n=268), black dots are Brazilian ports of entry (n=34), and a line the direct distance of an active route (n=1088).

Figure 1: Plants, ports, and routes

with the Principal Ports data of the United States Army Corps of Engineers (USACE). The final sample consists of 71 large ports, among which 32 ship to Brazil. Appendix B.2 provides port-level summary statistics.

Global port-level traffic. To recover global port-level traffic, I use the daily indicators of port and trade activity provided by the IMF PortWatch. The data contains daily count of port calls, estimates of import and export volumes (in TEU) disaggregated by ship type (contained, dry bulk, general cargo, tankers, ro-ro) for 1666 global ports, from 2019 to 2023. I match 531 ports by name with the Brazilian bill of lading data, and use the daily port-level aggregates of imported and exported TEU volumes as a proxy for port traffic.[13]

Tropical cyclones tracks. I obtain information on tropical cyclones using the IBTrACS (International Best Track Archive for Climate Stewardship) database (Knapp et al., 2010). This database provides a comprehensive record of tropical storms and cyclones since 1841. It contains detailed characteristics of storm systems' positions and intensities, with a 3-hour temporal resolution and a 0.1° spatial resolution. I focus on all cyclones that occurred from 2014 to 2019 within a 200km buffer zone around mainland US coasts. Appendix B.4 provides summary statistics on cyclones' wind profiles.

Tropical cyclones climate. I obtain port-level current and future tropical cyclone cli-

[13]Data dowloaded from IMF PortWatch. The data is based on raw AIS data from the United National Global Platform. Port-level daily estimates are PortWatch team's calculations, based on the methodology described in Arslanalp et al. (2021).

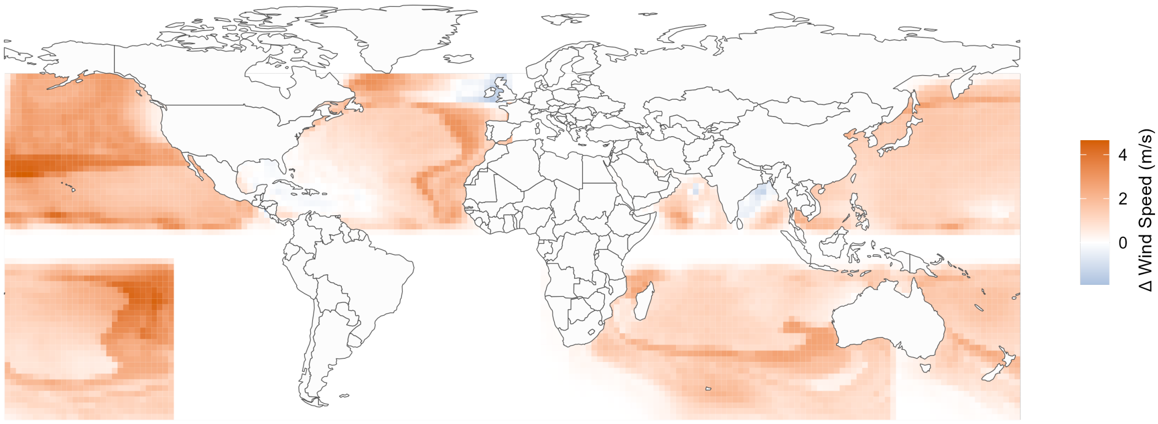

Figure 2: Present to RCP8.5: Δ Tropical Cyclone Windspeed

Notes: This map reports the change in expected windspeed induced by tropical cyclones, from the present-day scenario (1980-2015) to a RCP8.5 scenario (2015-2050). The calculations are based on windspeed and return periods for 10,000 years of synthetic cyclone tracks from the STORM model.

mates from the STORM model (Bloemendaal et al., 2020a,b). The data reports the maximum windspeed (meter/second) for a fixed set of return periods, recovered from 10,000 years of synthetic tropical cyclone tracks under present-day (1980-2015) and future climate scenario (2015-2050, RCP8.5/SSP5) at a 10km resolution. I calculate the expected windspeed in a 2° grid cell as the sum of maximum sustained windspeed weighted by the inverse of their return period (i.e. the probability of occurrence in 10,000 years). Figure 2 maps the global change in expected windspeed from tropical cyclone. Figure B.1 reports the raw data.

3 Empirical Evidence

3.1 Exposure to Tropical Cyclones

I proceed to describe the nature of the shocks I consider and how I measure the exposure of firms (and relationships) to tropical cyclones affecting maritime ports. I first describe how I define and measure the exposure of US ports to tropical cyclones. I then describe how I assign firm-to-firm relationships and their trading routes to these *treatments*.

Port condition ZULU and shocks to ports. Tropical cyclones may affect the operations of maritime ports in several ways (Verschuur et al., 2023a). Port critical infrastructure is at risk of damage under heavy rain, floods, and intense wind. To prevent the risk of infrastructure damage upon the arrival of a tropical cyclone within 72 hours, the US Coast Guards can issue a set of *port conditions* — i.e., measures restricting port operations — to guide ship operators in responding to tropical weather conditions. Importantly, these measures are issued upon the *projected* arrival of sustained gale-force winds (greater than 34 knots), leading ports to preemptively prepare for the arrival of a cyclone.[14] When the cyclone is projected to reach the port within 12 hours, the port condition ZULU is issued, closing the port to all vessel traffic. Appendix A provides an example of a Maritime Bulletin Safety Information, issued upon the arrival of Hurricane Milton at the port of Key West (October 2024, Florida). I use the port condition ZULU as a guide to define port disruptions induced by tropical cyclones.

Exhaustive information on the issuance of port conditions ZULU for all US ports is not easily accessible, nor is the actual experienced wind around ports during cyclone events. I therefore proxy disruptive tropical cyclone events by modeling the experienced wind speed around port locations, using the parametric model of Willoughby et al. (2006), adjusted for asymmetry using Chen (1994). The input of this cyclone profile simulation method is the IBTrACS data described in Section 2. The output is a vector of cyclone characteristics at the port level, including the maximum sustained wind speed experienced at the port location during the duration of the event. Figure 3 provides an example of the cyclone profile modeling procedure across the surface of the US for Hurricane Harvey (August 2017). For my baseline definition of a port-level shock, I use a threshold of experienced maximum wind speed of 28 knots.[15] This accounts for (i) noise in the modeling of experienced wind speeds and (ii) uncertainties regarding the trajectory of the cyclone and the projected wind speed models used by port authorities to inform the port conditions issuance decisions.[16] Importantly, I use the time of the first ever recorded information on the cyclone as the time of the shock. This corresponds to the time at which the weather agency discovered the cyclone anomaly and therefore helps avoid any anticipation of the cyclone by economic agents in a difference-in-difference setting. Table B.6 reports summary statistics on tropical cyclones.

Measuring exposure to port disruptions. I define the treatment variable $E_{i,t} = 1$ when the unit of analysis i is *exposed* to a tropical cyclone at period t, where t corresponds to the birth period of the cyclone, and 0 otherwise.

For port-level analyses, i corresponds to US ports, and t represents days. Ports are assigned to treatment whenever they are exposed to a maximum sustained wind speed above the 28-knot threshold. For relationship-level analyses, i corresponds to a pair (b, s), where b is a Brazilian buyer and s is a foreign supplier, and t represents months. Assigning firm pairs to treatment poses an additional challenge, as the bill of lading data only records existing shipments but does not contain information about delayed

[14] The knot is a unit of speed corresponding to one nautical mile per hour. Sustained gale-force winds approximately correspond to wind speeds greater than 63 kilometers per hour, or 39 miles per hour.

[15] This corresponds to 52 kilometers per hour, or 32 miles per hour.

[16] I reproduce my main results using higher thresholds (34 and 41 knots) in Appendix C.2.

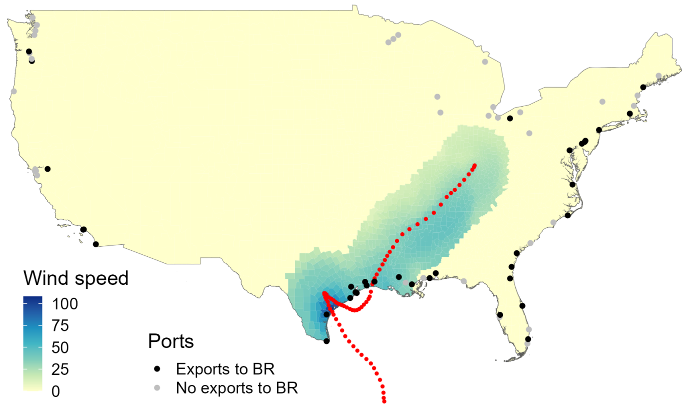

Figure 3: Wind speed profile of hurricane Harvey

Notes: This map shows the maximum sustained wind speed experienced by US counties during Hurricane Harvey (23 August to 02 September 2017). The red dots represent the eye of the hurricane across its lifespan (IBTrACS). Wind speed is modeled using the method of Willoughby et al. (2006), adjusted for asymmetry using Chen (1994). Black dots indicate US ports that export to Brazil in the Brazilian bill of lading data. Grey dots represent US ports that do not export to Brazil.

or canceled shipments due to port disruptions. To circumvent this issue, I assign a pair (b, s) to treatment if I observe any shipment between this pair of firms through an exposed port within a 6-month window prior to the cyclone event.[17] Therefore, a relationship is considered treated even if only a small proportion of its shipments transit through an exposed port.[18] For relationship-route-level analyses, i corresponds to a triplet (b, s, r), where b is a Brazilian buyer, s is a foreign supplier, r is a port of exit-to-port of entry maritime route, and t represents months. I assign a triplet (b, s, r) to treatment if I observe any shipment between this pair of firms through a route where the port of exit is an exposed port within a 6-month window prior to the cyclone event.

3.2 Tropical Cyclones, Maritime ports, and Supply Chain Disruptions

I leverage the quasi-random timing and location of tropical cyclones to examine how (i) port operations, (ii) firm-to-firm trade, and (iii) route choices are affected by weather shocks. The empirical setting I consider poses several challenges to estimation. First, the treatment is staggered, and the treatment effect is most likely heterogeneous across groups and over time. Tropical cyclones may affect ports that are more or less pre-

[17] I reproduce my main results using alternative exposure windows (12 months, 24 months, all months) in Appendix C.3.

[18] This is an important assumption, as the effect is likely to be larger for relationships that transit a large proportion of their shipments through exposed ports. The use of a binary treatment, as opposed to a continuous one, is constrained by the LP-DiD estimator.

pared and have different recovery abilities. Furthermore, treated relationships may differ across unobservable factors that affect their duration and ability to recover from shocks, such as age, specificity of inputs, etc. Recent work has demonstrated that two-way fixed-effect event-study estimators are biased in this case (Borusyak et al., 2024). Second, the treatment is non-absorbing: ports, and therefore relationships, can be treated multiple times while recovering in between. Third, the treatment is most likely continuous, depending on the magnitude of the cyclone events or the exposure to weather disasters.[19] Fourth, in order to disentangle the effect of the cyclone events on ports from the effects on firms themselves, I need to control for a large set of fixed effects.

I partially address these concerns by using the local-projection difference-in-difference estimator proposed by Dube et al. (2023) throughout the empirical exercise. The estimator allows for recovering interpretable average treatment effect estimates in a staggered design, with dynamic and heterogeneous treatment effects. It accommodates non-absorbing treatments under an assumption of effect stabilization and is computationally efficient, even with a large number of fixed effects.

3.2.1 Port-level disruptions

I first document that tropical cyclones temporarily affect the operations of US ports that ship to Brazil. I construct two daily measures of port activity from the US bill of lading data. The first outcome of interest — the extensive margin of port operations — is a binary variable that takes the value 1 if no vessels exporting goods were recorded during day t, i.e., the port is *closed*. The second outcome of interest — the intensive margin of port operations — is the log number of establishments that export through port p on day t, conditional on the port being open. The sample consists of all US ports that export at least once to Brazil (as recorded in the Brazilian bill of lading data). I consider the following local projection difference-in-difference specification to estimate the effect of cyclones on port activity:

$$y_{p,t+h} - \frac{1}{15}\sum_{\tau=t-15}^{t-1} y_{p,\tau} = \beta_h \Delta E_{p,t} + \alpha^h_{p,y(t)} + \alpha^h_{p,m(t)} + \varepsilon^h_{p,t}\,, \tag{1}$$

where $y_{p,t+h}$ corresponds to the outcome of interest for a port p, h days after the port received treatment on day t. The regression controls for port-year and port-calendar month fixed effects, absorbing port-specific seasonality and yearly fluctuations in activity. Standard errors are clustered at the port level. Daily port-level outcomes show high volatility, and choosing the relative period $t-1$ as the baseline can lead to noisy

[19] Ports may rely on a set of critical infrastructure to operate, e.g., nearby power grids or entrepôts, with variation in exposure to weather disasters (Verschuur et al., 2023a). Firms exhibit varying degrees of reliance on high-risk routes for the delivery of goods.

estimates, even with the assumption of no anticipation. I therefore choose a specification in which the long difference of the outcome variable is taken relative to its average value over a 15-day interval before t, instead of relative to $t-1$.[20] As ports may be affected by multiple cyclone events within a month, the sample is restricted to observations that are either:

$$\begin{cases} \text{newly treated} & E_{p,t} = 1,\ E_{p,t-j} = 0 \text{ for } 1 \leq j \leq 15, \\ \text{or clean control} & \Delta E_{p,t-j} = 0 \text{ for } -h \leq j \leq 15. \end{cases}$$

That is, the effect of treatment is assumed to stabilize after 15 days, and observations that experience a change in treatment status between $t-15$ and $t-1$, or between $t+1$ and $t+h$ are excluded from the estimation sample. Figure 4a shows the results of estimating Equation (1) on the extensive margin of port activity, for a 15-day window before and after the shocks. The effect of port exposure to cyclones is a 3- to 4-day increase in the probability of closing the port before ports recover operations. The effect corresponds to a 41% increase in the probability of closing within the exposure window.[21] The recovery period shows signs of a temporary decrease in the probability of closing, likely linked to the port working full time to catch up with planned shipments. Figure 4b shows that, when ports do not close, the number of exporting firms jumps as the cyclone is announced and decreases around the landfall.

3.2.2 FIRM-TO-FIRM DISRUPTIONS

I then document the effect of port exposure to cyclones on firm-to-firm trade. I am mainly interested in the extensive margin of firm-to-firm trade, i.e., in supply chain composition. My first outcome of interest is a monthly measure of relationship activity, defined as a binary variable taking the value 1 for a positive number of shipments within the relationship (b, s) at month t, and 0 otherwise. Relationship activity is conditioned on the entry and exit of the relationship, respectively defined as the first and last recorded shipments between b and s.[22] Given that such a measure may underestimate the effect of cyclones if relationships terminate, I construct a measure of relationship termination, a binary variable taking the value 1 at the month of the

[20] This is referred to as the 'pre-mean-differenced' estimator in Dube et al. (2023).

[21] The unconditional probability of port closing is 0.58. The duration of the effect is consistent with the findings of Verschuur et al. (2020). Reviewing the effect of natural disasters on port operations using vessel tracking data, they find a median disruption duration of six days. In many instances, port operations *recapture*, i.e., port productivity increases immediately after the event to reduce further delays in shipments.

[22] This avoids making comparisons between poorly defined *potential* relationships, i.e., before the recorded first activity of the relationships. When the first recorded shipment is observed within the first year of the sample, I consider that the relationship enters during the first period of the sample. I treat the exit of relationships analogously, when the last recorded sale is observed within the last year of the sample.

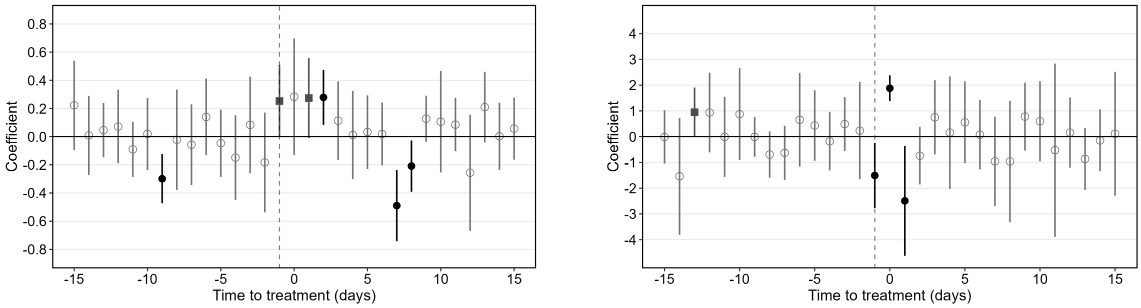

(a) Probability of closing (b) Log number of exporting firms

Figure 4: The impact of exposure to cyclones on port activity

Notes: These panels plot the effect of exposure to tropical cyclones on daily port-level outcomes, as specified by Equation (1). The outcome of Panel 4a is a binary variable, taking value 1 if no vessels exported goods in period t (port closing), 0 otherwise. The outcome of Panel 4b is the log number of exporting plants using the port in period t, conditioning on at least one vessel exporting goods. Regressions include port-year and port-month fixed effects. The sample consists of all geolocalized US ports, which ship to Brazil from 2014 to 2019. Standard errors are clustered at the port level. The bars correspond to 95% confidence intervals. Black dots are point estimates significant at the 5% level, gray squares are point estimates significant at the 10% level, and empty dots are point estimates non-significant at the 10% level.

last recorded shipment of the relationship, and 0 otherwise.[23] To estimate the effect of cyclones affecting maritime ports on firm-to-firm trade, I consider the following local projection difference-in-difference specification:

$$y_{bs,t+h} - y_{bs,t-1} = \beta_h \Delta E_{bs,t} + \alpha^h_{s,t} + \alpha^h_{b,t} + \varepsilon^h_{bs,t} \,, \tag{2}$$

where $y_{bs,t+h}$ corresponds to the outcome of interest for a buyer-supplier relationship (b,s), h months after the relationship received treatment at month t. The regression controls for buyer-month and supplier-month fixed effects. These fixed effects absorb supplier- or buyer-specific shocks. This is particularly important to disentangle the effect of cyclones on the ports that the relationships use while removing the effect of cyclones on the suppliers themselves. Standard errors are clustered at the buyer level. As relationships may be affected by multiple cyclone events, the sample is restricted to observations that are either:

$$\begin{cases} \text{newly treated} & E_{bs,t} = 1,\ E_{bs,t-j} = 0 \text{ for } 1 \leq j \leq 6, \\ \text{or clean control} & \Delta E_{bs,t-j} = 0 \text{ for } -h \leq j \leq 6. \end{cases}$$

That is, the effect of treatment is assumed to stabilize after 6 months, and observations that experience a change in treatment status between $t-6$ and $t-1$, or between $t+1$ and $t+h$, are excluded from the estimation sample. Figure 5a reports the estimation of Equation (2) on relationship activity, 6 months before and 12 months after the

[23]This measure is similar to that of Martinez (2024).

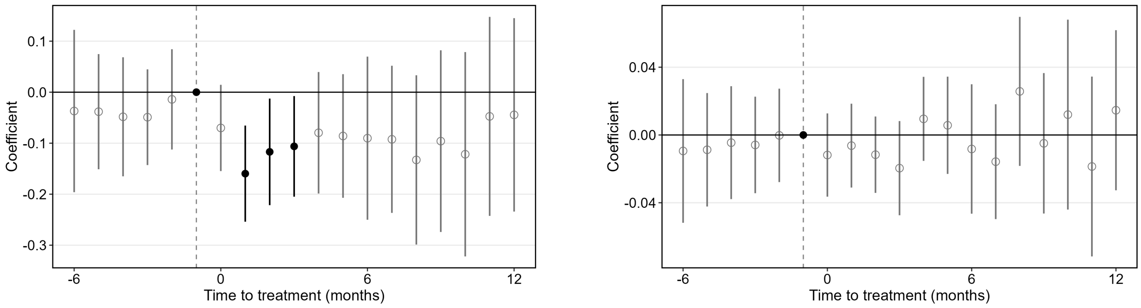

(a) Relationship activity (b) Relationship termination

Figure 5: The impact of port exposure to cyclones on firm-to-firm relationship

Notes: These panels plot the effect of port exposure to tropical cyclones on monthly firm-to-firm-level outcomes, as specified by Equation (2). The outcome of the left panel (a) is a binary variable, taking the value 1 if at least one shipment is observed for the trading pair at month t (active relationship), and 0 otherwise. Relationship activity is conditioned on the entry and exit of the relationship. The outcome of the right panel (b) is a binary variable, taking the value 1 if an observed shipment at month t is the last observable shipment of the trading pair (relationship termination), and 0 otherwise. Regressions include buyer-time and supplier-time fixed effects. Standard errors are clustered at the buyer level. The bars correspond to 95% confidence intervals. Black dots are point estimates significant at the 5% level, gray squares are point estimates significant at the 10% level, and empty dots are point estimates non-significant at the 10% level.

shock. Results suggest that port exposure to cyclones has a three-month temporary effect on the extensive margin of firm-to-firm trade, before a full recovery of the probability of activity (conditioning on relationships that do not terminate). The effect is largest one month after the birth of the cyclone, corresponding to a 36% decrease in the probability of trading for treated relationships compared to untreated relationships.[24] Figure 5b reports the estimation of Equation (2) on relationship termination within a similar time window. Results show no particular signs of an increase in relationship termination, suggesting that the shocks are not large enough to permanently recompose supply chains around the shocks' timing. In addition, I find no significant effect on the intensive margin of trade, measured as the log number of shipments, the log total weight, or the log total volume, conditional on active relationships. Figure C.1 reports results of the intensive margin specifications.

3.2.3 Route choice

I finally turn to the effect of port exposure to cyclones on the choice of routes that firms take when shipping goods. Having already established that firms decrease trade around the time of the cyclone, I seek to understand whether the choice of the route is an adaptation margin when firms keep trading after being treated. I restrict attention

[24]The unconditional probability of relationship activity in the sample is 0.35.

to all relationships that are treated throughout the sample.[25] The outcome of interest is a monthly measure of the extensive margin of route activity, a binary variable taking the value 1 for a positive number of shipments between b and s, using route r, and 0 otherwise. Route activity is conditioned on (b,s) being active at t, so as to disentangle route activity from relationship activity. I also consider an intensive margin outcome, the log share of shipments between b and s using route r, conditioned on route activity. I consider the following local projection difference-in-difference specification:

$$y_{bsr,t+h} - y_{bsr,t-1} = \beta_h \Delta E_{bsr,t} + \alpha^h_{bs,t} + \alpha^h_{p_d(r),t} + \varepsilon^h_{bsr,t} \,, \tag{3}$$

where $y_{bsr,t+h}$ corresponds to the outcome of interest for a relationship-route (b,s,r), h months after the relationship received treatment at month t. The regression controls for relationship-month and port of destination-month fixed effects. As such, I restrict comparisons to within-relationship route choice, holding constant the port of destination. I aim to isolate the choice of the port of origin to ship goods, given that only ports of origin are potentially treated. Standard errors are clustered at the relationship level. As routes within a relationship may be affected by multiple cyclone events, the sample is restricted to observations that are either:

$$\begin{cases} \text{newly treated} & E_{bsr,t} = 1, \; E_{bsr,t-j} = 0 \text{ for } 1 \leq j \leq 6, \\ \text{or clean control} & \Delta E_{bsr,t-j} = 0 \text{ for } -h \leq j \leq 6. \end{cases}$$

That is, the effect of treatment is assumed to stabilize after 6 months, and observations that experience a change in treatment status between $t-6$ and $t-1$, or between $t+1$ and $t+h$, are excluded from the estimation sample. Figure 6a reports the estimation of Equation (3) on route activity, 6 months before and 12 months after the shock. Results suggest that, conditioning on relationship activity, port exposure to cyclones has a long-lasting effect on route choice. Twelve months after the shock, the effect corresponds to a 45% decrease in the probability of trading through the exposed route compared to untreated routes within the same relationship.[26] Figure 6b reports the estimation of Equation (3) on the log share of shipments through the route. Results show only a slight effect (significant at the 90% level) on the intensive margin of route activity.

[25]The sample consists of 1,906 relationships. Table B.4 reports summary statistics for this sample at the relationship-route level.

[26]The unconditional probability of route activity in the sample is 0.40.

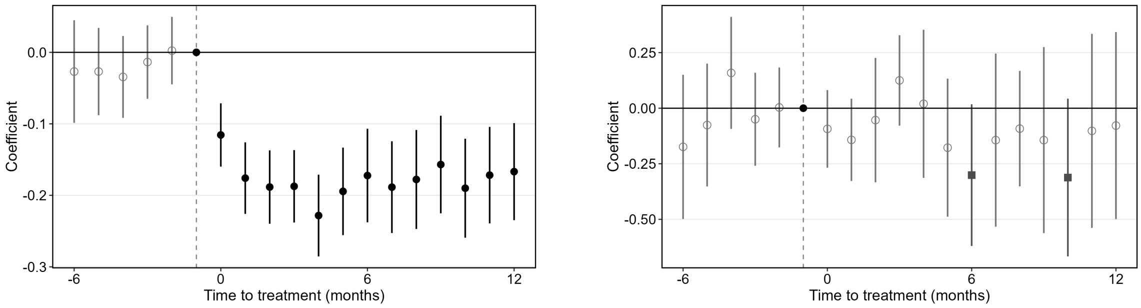

(a) Route activity

(b) Log share of shipments

Figure 6: The impact of port exposure to cyclones on route choice

Notes: These panels plot the effect of port exposure to tropical cyclones on monthly firm-to-firm-route-level outcomes, as specified by Equation (3). The outcome of the left panel (a) is a binary variable, taking the value 1 if at least one shipment is observed for the trading pair through route r at month t (active route), and 0 otherwise. Route activity is conditioned on the activity of the firm-to-firm relationship. The outcome of the right panel (b) is the log share of shipments of the relationship using route r. The log share of shipments is conditioned on the activity of the route. Regressions include relationship-time and port of destination-time fixed effects. Standard errors are clustered at the relationship level. The bars correspond to 95% confidence intervals. Black dots are point estimates significant at the 5% level, gray squares are point estimates significant at the 10% level, and empty dots are point estimates non-significant at the 10% level.

4 Theory

In this section, I develop a theory of spatial production network formation with endogenous trade costs and weather shocks to trade infrastructure. The model rationalizes my empirical findings: (i) tropical cyclones affect the operation of maritime ports and induce firm-to-firm trade disruptions, and (ii) firms adapt to these disruptions by re-routing trade, even after the recovery of port activities. I use the model to perform counterfactual simulations on a climate change scenario and infrastructure-related adaptation policies.

To parsimoniously capture empirical evidence on the impacts of trade infrastructure exposure to weather disasters on global supply chains, I assume that, in a production network environment similar to that of Oberfield (2018), firms take a joint sourcing and routing decision over the beliefs they form on factory-gate costs and trade costs.[27] Trade costs are endogenous to traffic congestion, as in Allen and Arkolakis (2022), and for maritime routes include the costs of using maritime port infrastructure, which is potentially affected by weather disasters. Firms are perfectly informed about the underlying distribution of weather-related risks to port infrastructure.

The model is able to form predictions that are not testable in the reduced-form empirical evidence in Section 3. First, the model incorporates traffic congestion, which

[27] I draw from the model of endogenous production network formation under idiosyncratic and aggregate weather disaster risks presented in Balboni et al. (2024). Chen et al. (2023) proposes a related model in which technology compatibility between firms shapes the marginal costs of inputs. I extend this class of models with a geography, endogenous trade costs, and transportation-related weather risks.

likely impacts trade costs in the long run. Section 3.2 shows that firms adapt by redirecting trade through alternative routes long after the ports recover from the shocks. If traffic congestion increases the cost of using these alternative routes, such adaptation mechanisms may, in turn, distort bilateral components of sourcing shares and affect the aggregate impacts of infrastructure exposure to weather disasters. Second, while the empirical results describe the reactions to single weather events, they do not address a local shift in the *distribution* of weather events — which is a hallmark of climate change. The model accommodates such a counterfactual scenario, with the assumption that a shift in the perfectly-informed beliefs of firms over the distribution of weather disasters is akin to a sequence of realized events through which firms update information on the probability set of extreme weather events.[28]

4.1 Environment

The economy consists of a discrete set $\mathcal{N}$ of cities (indexed by n or n'), each populated with a continuum $M_n \in \{M_n\}_{n\in\mathcal{N}} \equiv \mathcal{M}$ of firms, and an exogenous measure of households $L_n \in \{L_n\}_{n\in\mathcal{N}} \equiv \mathcal{L}$. Each city is endowed with a fundamental productivity $a_n \in \{a_n\}_{n\in\mathcal{N}} \equiv \mathcal{A}$. Some cities contain port infrastructure (port-cities), allowing for trade across cities that are not connected by land. The set of port-cities is denoted $\mathcal{P}$. Both cities and ports are connected through a *transportation network*, i.e., a matrix of bilateral trade frictions $\delta_{ll'} \in \{\delta_{ll'}\}_{l,l'\in\mathcal{N}\cup\mathcal{P}\times\mathcal{N}\cup\mathcal{P}} \equiv \mathbf{T}$ incurred from moving directly from a location (a city or a port, indexed by l or l') to another. The transportation network is a function of endogenous variables (traffic) and exogenous ones (distance and capacity). Cities are distant from each other, with a bilateral measure of distance $\epsilon_{nn'} \in \{\epsilon_{nn'}\}_{n,n'\in\mathcal{N}^2} \equiv \mathcal{D}$. Each port has a capacity denoted $K_p \in \{K_p\}_{p\in\mathcal{P}} \equiv \mathcal{K}_p$ (e.g., port berths). Cities are connected via a countable set of routes $\mathcal{R}$, allowing trade in intermediate inputs.

Households. Households in city n inelastically supply labor l_i to local firms and consume a bundle of differentiated final goods supplied by local firms:

$$q_n = \left(\int_{i\in M_n} q_i^{\frac{\sigma-1}{\sigma}} di \right)^{\frac{\sigma}{\sigma-1}}, \tag{4}$$

where q_i is the quantity of final goods supplied by firm $i \in M_n$ to households, and $\sigma > 1$ is the elasticity of substitution across varieties of final goods supplied in city n. I assume no trade in final goods and no migration across cities.[29] Households are

[28]Note that, although static, the model can also serve as a description of the immediate aftermath of a weather disaster and therefore can accommodate the dynamic — but short-lived — disruptions described in Section 3.

[29]These are restrictive assumptions but ones that map directly to the model studied in Section 3, and

subject to the budget constraint:

$$\int_{i \in M_n} q_i p_i di = w_n + \Pi_n, \tag{5}$$

where p_i is the price charged by firm i to households for final goods, w_n is the wage rate in city n, and Π_n are per-capita profits rebated from firms to households in city n.

Firms. Firms' production process involves combining local labor and perfectly substitutable intermediate inputs supplied by other firms along different routes. Firms are faced with a mass of potential suppliers located in all cities (including locally) and a set of delivery routes. A specific combination of labor, input, and delivery route yields a 'technique' of production, defined over a supplier-buyer match ϕ and a delivery route r:

$$y_i(\phi, r) = \chi a_{n(i)} l_i^{1-\alpha} (z(\phi) x_i(\phi, r))^{\alpha}, \tag{6}$$

where l_i is the amount of labor used by firm i, $x_i(\phi, r)$ is the amount of intermediate inputs supplied through route r and yielding the match-specific input-augmenting productivity $z(\phi)$, and $a_{n(i)}$ is city-specific productivity shifter.[30]

Firms choose the technique that yields the minimum marginal cost of production, at which they sell their goods to other firms — i.e., buyers have full bargaining power (see Oberfield (2018)). Firms engage in monopolistic competition when selling final goods to local households. Trade in intermediate inputs is subject to route-specific iceberg costs such that, for each unit to be used as an input in production, $\tau_{n(j)n(i)}(r) \geq 1$ units must be shipped from the supplier's city $n(j)$ to the buyer's city $n(i)$ using route r. The factory-gate price (marginal cost) of production using technique (ϕ, r) is such that:

$$c_i(\phi, r) = \frac{w_{n(i)}^{1-\alpha}}{a_{n(i)}} \left(\tau_{n(j)n(i)}(r) \frac{c_j(\phi)}{z(\phi)} \right)^{\alpha}, \tag{7}$$

where $c_j(\phi)$ is the marginal cost of inputs from supplier j. I make two functional form assumptions on firms, which allow for a tractable characterization of the equilibrium.

ASSUMPTION 1. *For any firm i in city n, the number of potential suppliers $j \in M_{n'}$ that i can choose from, and that yield a match productivity $z > \bar{z}$, is distributed Poisson with mean $a_{n'} \bar{z}^{-\xi}$, where $a_{n'}$ is the fundamental productivity of firms in city n'.*

Assumption 1 describes the distribution of match-specific productivity among the techniques available to a firm in n, and idiosyncratic productivity. The parameter ξ determines the tail behavior of the distribution of match-specific productivity draws (Oberfield, 2018; Chen et al., 2023; Balboni et al., 2024). A higher value of ξ implies that

to the fact that I only observe firm-related transactions in the bill of lading data.

[30] χ is a normalizing constant equal to $\alpha^{-\alpha}(1-\alpha)^{-(1-\alpha)}$.

the draws are, on average, more similar, making a buyer more inclined to substitute to an alternative supplier when route-level or factory-gate-level costs increase.

Shipping. Firms from city n can ship to any other city. However, shipment may be indirect, as some cities are not directly connected (e.g., by a direct road or shipping line). Shipping routes are comprised of a countable set $\mathcal{B}_r$ of legs, with $|\mathcal{B}_r| - 1$ stops from origin n ($k = 1$) to destination n' ($k = |\mathcal{B}_r|$). Each stop may be a port or a non-port city. Each stop involves iceberg direct transportation costs across all cities, as well as port-city-level trade costs. For a route r connecting n to n' through $|\mathcal{B}_r|$ legs, including $|\mathcal{P}_r|$ port cities, the trade costs are given by:

$$\tau_{n(j)n(i)}(r) = \prod_{k=1}^{|\mathcal{B}_r|} d_{r_{k-1},r_k} \prod_{m=1}^{|\mathcal{P}_r|} t_{p(r)_m}. \tag{8}$$

Following Ganapati et al. (2024), I allow for transportation costs to be a function of both endogenous and exogenous variables:

$$d_{r_{k-1},r_k} = d(\epsilon_{r_{k-1},r_k}), \quad t_{p(r)_m} = t(\Xi, K_{p(r)_m}) \times \theta_{p(r)_m}, \tag{9}$$

where ϵ_{r_{k-1},r_k} represents exogenous transportation costs, such as distance, Ξ is a matrix of traffic flows, $K_{p(r)_m}$ represents port-level infrastructure capacity, while $\theta_{p(r)_m}$ represents port-level weather-related wedges, with the following assumption:

ASSUMPTION 2. *Port-level wedges are randomly drawn from a Pareto distribution with c.d.f. $F_{p(r)}(\theta) = 1 - \theta^{-\psi_{p(r)}}$, for $\theta_{p(r)} \geq 1$.*

Assumption 2 describes the distribution of port-level wedges. With a higher shape parameter $\psi_{p(r)}$, firms will on average draw lower transportation cost wedges, as the tail of the distribution becomes thinner. This assumption ensures that transportation costs in Equation (8) remain tractable.

Sourcing and routing decisions. I first characterize the distribution of factory-gate costs.

PROPOSITION 1. *Under Assumption 1, the marginal cost distribution of firms in $M_{n'}$ is Weibull:*

$$P(c_i(\phi, r) > c) = \exp\left[-\left(a_{n'} w_{n'}^{\alpha-1}\right)^{\frac{\xi}{\alpha}} \left(\sum_n a_n \bar{c}_n^{-\xi} \sum_{r \in \mathcal{R}_{nn'}} \prod_{k=1}^{|\mathcal{B}_r|} d_{r_{k-1},r_k}^{-\xi} \prod_{m=1}^{|\mathcal{P}_r|} \bar{t}_{p(r)_m}^{-\xi} \right) c^{\frac{\xi}{\alpha}} \right], \tag{10}$$

$$\textit{where} \quad \bar{c}_n^{-\xi} = a_n^{\xi} w_n^{(\alpha-1)\xi} \left(\sum_{\tilde{n}} a_{\tilde{n}} \bar{c}_{\tilde{n}}^{-\xi} \sum_{r \in \mathcal{R}_{\tilde{n}n}} \prod_{k=1}^{|\mathcal{B}_r|} d_{r_{k-1},r_k}^{-\xi} \prod_{m=1}^{|\mathcal{P}_r|} \bar{t}_{p(r)_m}^{-\xi} \right)^{\alpha} \Gamma(1-\alpha), \tag{11}$$

$$\text{and} \quad \bar{t}^{-\xi}_{p(r)_m} = \int_1^\infty t^{-\xi}_{p(r)_m} dF_{p(r)_m}(\theta). \tag{12}$$

Proof. See Appendix D.1.

This result follows from the fact that, if the *effective* price of inputs for suppliers in all origin cities and delivering through any route is distributed Weibull, then the distribution of factory-gate prices of all firms i in destination n' is also distributed Weibull.[31] The production network structure affects the distribution of marginal costs through the factory-gate costs of the upstream suppliers, apparent in Equation (11) specifying the cost indices of downstream firms as a fixed point. The transportation costs, however, depart from similar models of production network formation (Chen et al., 2023; Balboni et al., 2024) by explicitly including the set of links and transportation infrastructure of which routes are composed. I characterize the joint sourcing and routing decisions of firms as a corollary to Proposition 1.

COROLLARY 1. *The probability that firm i in n' sources from route r connecting n to n' is:*

$$\pi_{i,r} = \frac{a_n \bar{c}_n^{-\xi} \prod_{k=1}^{|\mathcal{B}_r|} d^{-\xi}_{r_{k-1},r_k} \prod_{m=1}^{|\mathcal{P}_r|} \bar{t}^{-\xi}_{p(r)_m}}{\sum_{\tilde{n}} a_{\tilde{n}} \bar{c}_{\tilde{n}}^{-\xi} \sum_{r \in \mathcal{R}_{\tilde{n}n'}} \prod_{k=1}^{|\mathcal{B}_r|} d^{-\xi}_{r_{k-1},r_k} \prod_{m=1}^{|\mathcal{P}_r|} \bar{t}^{-\xi}_{p(r)_m}}. \tag{13}$$

Proof. See Appendix D.1.

Equation (13) represents the unconditional probability of choosing route r to source goods. Given that route r links destination n' to origin n, Equation (13) jointly specifies the sourcing city and the delivering route. Given that this probability is independent of firm i characteristics, $\pi_{i,r}$ is also the share of expenses of city n' in city n through route r. Aggregating the sourcing-routing shares across routes yields city-to-city bilateral trade shares, as shown in Corollary 2:

COROLLARY 2. *The bilateral trade share between n' and n is:*

$$\pi_{nn'} = \frac{a_n \bar{c}_n^{-\xi} \tau_{nn'}^{-\xi}}{\sum_{\tilde{n}} a_{\tilde{n}} \bar{c}_{\tilde{n}}^{-\xi} \tau_{\tilde{n}n'}^{-\xi}}, \tag{14}$$

$$\text{where} \quad \tau_{nn'} = \left(\sum_{r \in \mathcal{R}_{nn'}} \left(\prod_{k=1}^{|\mathcal{B}_r|} d^{-\xi}_{r_{k-1},r_k} \right) \left(\prod_{m=1}^{|\mathcal{P}_r|} \bar{t}^{-\xi}_{p(r)_m} \right) \right)^{-\frac{1}{\xi}}. \tag{15}$$

Proof. See Appendix D.1.

[31] I define the effective price of inputs delivered by supplier j through route r as

$$\lambda_j(\phi, r) = \frac{c_j}{z(\phi)} \prod_{k=1}^{|\mathcal{B}_r|} d_{r_{k-1},r_k} \prod_{m=1}^{|\mathcal{P}_r|} t_{p(r)_m}.$$

Equation (14) resembles one of traditional trade models, with the addition of production-network-affected marginal cost indices $\bar{c}_n$ and endogenous transportation costs. Equation (15) embodies my departure from trade modeling with endogenous routing (Allen and Arkolakis, 2022; Ganapati et al., 2024), with the addition of infrastructure-level costs.

Equilibrium transportation costs. Define the auxiliary matrix Δ as a $(|\mathcal{N}| + |\mathcal{P}|) \times (|\mathcal{N}| + |\mathcal{P}|)$ matrix, where $|\mathcal{N}|$ corresponds to the number of cities (port- or non-port cities), and $|\mathcal{P}|$ the number of port cities. Each of the first $|\mathcal{N}|$ rows and columns of Δ corresponds to a city, while each of the last $|\mathcal{P}|$ rows and columns of Δ corresponds to a port. Denoting both cities and ports as *locations*, indexed l or l', the (l, l') entry $\delta_{ll'}$ of Δ is 0 if l and l' are not directly connected. If both locations are connected and l' is a port, then $\delta_{ll'} = d_{ll'}^{-\xi} \bar{t}_{l'}^{-\xi}$. If both locations are connected and l' is not a port, then $\delta_{ll'} = d_{ll'}^{-\xi}$. It follows that the city-to-city transportation costs are given by the Leontiev inverse of the auxiliary matrix Δ:

$$[\tau_{nn'}] = \left[(I - \Delta)^{-1}\right]^{\circ\left(-\frac{1}{\xi}\right)}. \tag{16}$$

The conditional probability that a good passes through port p, given origin n and destination n', is:[32]

$$\pi(p|nn') = \left(\frac{\tau_{np}\tau_{pn'}}{\tau_{nn'}}\right)^{-\xi}, \tag{17}$$

Using these port-level conditional probabilities, I characterize traffic as the total value of goods that transit through ports:

$$\Xi_p = \sum_n \sum_{n'} \left(\tau_{np}\tau_{pn'}\tau_{nn'}^{-1}\right)^{-\xi} X_{nn'}, \tag{18}$$

where $X_{nn'}$ is the total trade value from n' to n.

Closing the model. Appendix D.2 completes the description of the model environment. The model closes with a good market clearing condition, which requires trade in intermediate inputs to be balanced.

Equilibrium. Appendix D.3 formally defines the general equilibrium of the model with traffic congestion, and provides the system of equation that characterizes it. Appendix D.4 provides the numerical algorithm implemented to recover counterfactual equilibria.

[32] Here, I follow Allen and Arkolakis (2022) and Ducruet et al. (2024).

5 Model Parameterization and Calibration

The aim is to estimate key parameters of the model using bill of lading microdata when feasible, and calibrate the model at a fine spatial granularity. I need to recover the following parameters and fundamentals: the measures of labor (L_n), the measures of firms (M_n), fundamental city-level productivity a_n, port capacity (K_p), transportation costs elasticity to distance (λ_1), elasticity to traffic (λ_2), elasticity to port-level capacity (λ_3), port-level weather dispersion (ψ_p), final goods elasticity of substitution (σ), the intermediate input share (α), and the dispersion of match-specific productivity (ξ). Table 2 summarizes the provenance or procedure to obtain the calibrated parameters and fundamentals.

5.1 Estimating transportation costs

I aim at recovering a set of transportation costs that account for the effect of traffic, port capacity, and weather risk. I parametrize the general formulation of transportation costs in Equation (9) as:

$$d_{nn'}^{-\xi} = \epsilon_{nn'}^{\lambda_1} \quad \text{, and} \quad \bar{t}_p^{-\xi} = \Xi_p^{\lambda_2} K_p^{\lambda_3} \frac{\psi_p}{\psi_p + \xi}, \tag{19}$$

where λ_1 is the elasticity of link-level costs to distance, λ_2 is the elasticity of port-level costs to port traffic, and λ_3 is the elasticity of port-level costs to port capacity.[33] To estimate the parameters affecting transportations costs, I use a reduced-form analog of route-level bilateral trade shares described in Corollary 1:

$$\begin{aligned} \log(\pi_{n_d,r,t}^{weight}) = \alpha_{n_o n_d,t} + \alpha_{p_d,t} &+ \alpha_1 \log(Distance_r) \\ &+ \alpha_2 \log(\Xi_{p_o,t}^{TEU}) \\ &+ \alpha_3 \log(K_{p_o}^{TEU}) \\ &+ \alpha_4 \log(CycloneRisk_{p_o}) \\ &+ \varepsilon_{n_d,r,t}. \end{aligned} \tag{20}$$

I bring Equation (20) to the data by constructing a microdata equivalent of route-level bilateral trade share from Brazilian bill of ladings. That is, $\pi_{n_d,r,t}^{weight}$ is defined the weekly share of shipment weight that destination location n_d sources through route r.[34] In the data, locations to refer GAUL1 sub-national units, while routes are approximated as the quadruplet $\{n_o, n_d, p_o, p_d\}$, where p_o and p_d are respectively the port of origin, and port of destination of shipments. The distance component of transportation costs is

[33] From Proposition 1 and the definition of port-level trade costs in Equation (9), $\bar{t}_p^{-\xi} = t(\Xi, K_p)^{-\xi} \int_1^\infty \theta_p^{-\xi} dF_p(\theta)$. Assumption 2 implies that $\int_1^\infty \theta_p^{-\xi} dF_p(\theta) = \psi_p/(\psi_p + \xi)$, and I parametrize $t(\Xi, K_p)^{-\xi} = \Xi_p^{\lambda_2} K_p^{\lambda_3}$.

[34] I use weight instead of value to prevent misreporting of shipment values to bias the results.

approximated as the least-cost distance over land and sea traveled by the goods from supplier origin to buyer destination, traveling through p_o and p_d. I use weekly estimates of total TEU volumes transiting through ports from PortWatch to proxy port-level traffic. Port capacity is proxied as the maximum daily TEU volume ports process throughout the sample. I proxy cyclone risks with expected windspeed at the port, as reported in the STORM data (Figure B.1a).[35] Origin-destination-time fixed effects control for any origin or destination general equilibrium terms in Equation (13). Regressing route-level bilateral trade share on port traffic causes for endogeneity concerns, as both are by definition positively correlated in Equation (18). Port of destination-time fixed effects partially alleviate this concerns, as port traffic and capacity elasticities are only estimated on port of origins. To further address endogeneity issues, I restrict the sample of ports of origin to US, China, and EU28 ports - whose weekly traffic are arguably exogenous to Brazilian-bound shipments.

Table 1 reports the results of the estimation. Conditional on port capacity, a 1% increase in port traffic reduces route-level bilateral trade shares by 0.25%. Assuming a widely used trade elasticity of $\xi = 4$, this results in a 0.06% increase in port-level trade costs.[36] On the other hand, a 1% increase in port capacity decreases port-level trade costs by 0.11%, indicating the presence of scale economies.[37] Furthermore, results suggest that a 1% increase in cyclone risks decreases route-level bilateral trade shares by 0.06%.

5.2 Fundamentals and economy-wide parameters.

Parameters from the literature. I follow Castro-Vincenzi (2024) by setting $\sigma = 2$, and Ganapati et al. (2024) by setting $\xi = 4$. I set the intermediate input share to $\alpha = 0.8$ following Balboni et al. (2024). (*A discussion about the selected parameters is in progress.*)

Fundamentals. The model is calibrated at the GAUL1 unit. I calibrate GAUL1-level population from the Gridded Population of the World (GPW) data provided by NASA. The data model the distribution of human population on a continuous global raster surface and allow recovery of population estimates at a 0.1° spatial resolution. Measures of firms are inferred from the Orbis by Bureau van Dijk dataset, providing data on companies worldwide, including firm counts at sub-national levels. I assign the ports in PortWatch to each GAUL1 unit, and use the maximum daily TEU traffic as a

[35] Formally, I parametrize $\frac{\psi_p}{\psi_p + \xi} = CycloneRisk_p = (1 + windspeed_p)^{\lambda_w}$, where $windspeed_p$ is computed as the yearly mean expected windspeed in cells within a 50km radius of the port, and λ_w is the elasticity of transportation costs to expected windspeed.

[36] By comparison, Allen and Arkolakis (2022) find an elasticity of traffic flow (per lane) to transportation cost of 0.09 in the US highway system.

[37] Given the high observed correlation between port level traffic and port capacity, this fact is consistent with the findings of Ganapati et al. (2024), who document scale economies in the maritime network, although not disentangling traffic from capacity.

Table 1: Estimation of transportation costs

Dep. var: Log $\pi^{weight}_{n_d,r,t}$	(1)	(2)
Log Distance	-0.19***	-0.48***
	(0.06)	(0.09)
Log Port Traffic (TEU)	-0.17***	-0.25***
	(0.04)	(0.06)
Log Port Origin Capacity	0.34***	0.42***
	(0.05)	(0.07)
Log Cyclone Risk	-0.07***	-0.06**
	(0.02)	(0.02)
Ports	All	US+CN+EU28
Fixed-effects		
Destination-Origin-Week	Yes	Yes
Port Destination-Week	Yes	Yes
Observations	33,702	23,248
Adjusted R^2	0.55	0.54

Note: This table reports the estimation of transportation costs on route-level bilateral trade shares (measured in weight of shipments), as specified in Equation (20). Column (2) restricts the sample to ports of origin from the US, China, and the EU28. Signif. Codes: ***: 0.01, **: 0.05, *: 0.1.

Table 2: Calibration of parameters and fundamentals

Parameters	Description	Source/Procedure
Panel A: Parameters from related literature		
$\sigma = 2$	Final goods CES	Castro-Vincenzi (2024)
$\alpha = 0.8$	Intermediate input share	Balboni et al. (2024)
$\xi = 4$	Trade elasticity	Ganapati et al. (2024)
Panel B: Calibrated parameters		
$\lambda_1 = -0.48$	Distance elasticity	Section 5.1
$\lambda_2 = -0.25$	Traffic elasticity	Section 5.1
$\lambda_3 = 0.42$	Capacity elasticity	Section 5.1
Fundamentals	**Description**	**Source/Matched moments**
Panel C: Calibrated fundamentals		
$\mathcal{N}$	Cities	Aggregation at GAUL1 level
$\mathcal{P}$	Port-cities	IMF PortWatch
$\mathcal{L}$	Population	NASA GPW
$\mathcal{A}$	City-level productivity	Matched to Rossi-Hansberg and Zhang (2025)
$\mathcal{D}$	Distance	Eurostat SeaRoute & OpenStreetMap
$\mathcal{K}_p$	Port capacity	IMF PortWatch
$\{\psi_p\}_{p\in\mathcal{P}}$	Weather wedge	Section 5.1

measure of port capacity. Distances between GAUL1 unit centroids are calculated as shortest road paths from the OpenStreetMap API. I use the Eurostat SeaRoute program to calculate shortest sea routes between ports. With the rest of the model parameters calibrated, I pin down city-level fundamental productivity by inverting the model, so as to recover the measure of local GDP provided by Rossi-Hansberg and Zhang (2025).

6 QUANTITATIVE RESULTS

This section is in progress and incomplete. In this section, I provide insights on the future quantitative exercises I will conduct. The aim is to perform climate change-related counterfactual simulations. The first counterfactual of interest pertains to increased risks of weather-related disruptions of maritime ports in a climate change scenario. The second counterfactual of interest is related to optimal infrastructure policy in the context of climate change.

Counterfactual simulations. I will conduct two main counterfactual simulations. First, I will infer the climate-change-induced increase in extreme wind events at the port level using the change in expected windspeed in the STORM data (Figure 2). The change in predicted wind conditions around port locations will provide my main counterfactual variable. Next, I will allow a social planner at the country level to reallocate port capacity K_p in the climate change scenario to redirect trade toward the least-affected ports using traffic congestion forces. This will indicate whether port capacity is misallocated in light of a climate change scenario that increases the risks of port disruptions.

7 CONCLUSION

This paper investigates the impacts of climate-induced disruptions on global supply chains, focusing on the role of disruptions to maritime trade infrastructure. Leveraging high-frequency data on firm-to-firm shipments and detailed cyclone activity, I provide empirical evidence on how extreme weather events affect port operations and reshape trade routes. My findings show that, while firm-to-firm relationships are only temporarily affected, routing decisions adapt significantly, reflecting a persistent reallocation of economic activity across transportation networks.

I further develop a quantitative model of spatial production networks incorporating endogenous transportation costs and congestion, offering a framework to evaluate the broader economic implications of climate-induced transportation disruptions. The model reveals spatial and welfare implications of climate risks to trade infrastructure for global trade, emphasizing the critical role of adaptive strategies and infrastructure resilience in mitigating adverse effects.

These findings have clear policy relevance. Investments in climate-resilient transportation networks can not only reduce the direct costs of disruptions but also alleviate secondary congestion effects on unaffected regions. Policymakers should prioritize adaptive strategies that account for dynamic firm behaviors and transportation network spillovers. While I only focus on maritime trade, future research could extend this analysis by incorporating additional modes of transport and leveraging the rich set of climate data currently available to study a wider array of extreme weather events, offering a more comprehensive picture of global supply chain vulnerability to climate risks affecting trade infrastructure.

References

T. Allen and C. Arkolakis. The Welfare Effects of Transportation Infrastructure Improvements. *The Review of Economic Studies*, 89(6):2911–2957, 2022. ISSN 0034-6527, 1467-937X. doi: 10.1093/restud/rdac001. URL https://academic.oup.com/restud/article/89/6/2911/6519332.

M. S. Arslanalp, M. R. Koepke, and J. Verschuur. Tracking Trade from Space: An Application to Pacific Island Countries. *IMF Working Papers*, Aug. 2021. URL https://ideas.repec.org//p/imf/imfwpa/2021-225.html. Number: 2021/225 Publisher: International Monetary Fund.

C. Balboni, J. Boehm, and M. Waseem. Firm Adaptation in Production Networks: Evidence from Extreme Weather Events in Pakistan. 2024.

J.-N. Barrot and J. Sauvagnat. Input Specificity and the Propagation of Idiosyncratic Shocks in Production Networks*. *The Quarterly Journal of Economics*, 131(3):1543–1592, Aug. 2016. ISSN 0033-5533, 1531-4650. doi: 10.1093/qje/qjw018. URL https://academic.oup.com/qje/article/131/3/1543/2461213.

A. Bilal and E. Rossi-Hansberg. Anticipating Climate Change Across the United States, June 2023. URL https://www.nber.org/papers/w31323.

J. Blaum, F. Esposito, and S. Heise. Input Sourcing under Supply Chain Risk:. *Working paper*, 2024.

N. Bloemendaal, H. de Moel, S. Muis, I. D. Haigh, and J. C. J. H. Aerts. Estimation of global tropical cyclone wind speed probabilities using the STORM dataset. *Scientific Data*, 7(1):377, Nov. 2020a. ISSN 2052-4463. doi: 10.1038/s41597-020-00720-x. URL https://www.nature.com/articles/s41597-020-00720-x. Publisher: Nature Publishing Group.

N. Bloemendaal, I. D. Haigh, H. de Moel, S. Muis, R. J. Haarsma, and J. C. J. H. Aerts. Generation of a global synthetic tropical cyclone hazard dataset using STORM. *Scientific Data*, 7(1):40, Feb. 2020b. ISSN 2052-4463. doi: 10.1038/s41597-020-0381-2. URL https://www.nature.com/articles/s41597-020-0381-2. Publisher: Nature Publishing Group.

C. E. Boehm, A. Flaaen, and N. Pandalai-Nayar. Input Linkages and the Transmission of Shocks: Firm-Level Evidence from the 2011 Tōhoku Earthquake. *The Review of Economics and Statistics*, 101(1):60–75, Mar. 2019. ISSN 0034-6535. doi: 10.1162/rest_a_00750. URL https://doi.org/10.1162/rest_a_00750.

K. Borusyak, X. Jaravel, and J. Spiess. Revisiting Event-Study Designs: Robust and Efficient Estimation. *Review of Economic Studies*, 91(6):3253–3285, Nov. 2024. ISSN 0034-6527, 1467-937X. doi: 10.1093/restud/rdae007. URL https://academic.oup.com/restud/article/91/6/3253/7601390.

G. Brancaccio, M. Kalouptsidi, and T. Papageorgiou. Geography, Transportation, and Endogenous Trade Costs. *Econometrica*, 88(2):657–691, 2020. ISSN 1468-0262. doi: 10.3982/ECTA15455. URL https://onlinelibrary.wiley.com/doi/abs/10.3982/ECTA15455. _eprint: https://onlinelibrary.wiley.com/doi/pdf/10.3982/ECTA15455.

G. Brancaccio, M. Kalouptsidi, and T. Papageorgiou. Investment in Infrastructure and Trade: The Case of Ports, May 2024. URL https://papers.ssrn.com/abstract=4843062.

V. M. Carvalho, M. Nirei, Y. U. Saito, and A. Tahbaz-Salehi. Supply Chain Disruptions: Evidence from the Great East Japan Earthquake*. *The Quarterly Journal of Economics*, 136(2):1255–1321, May 2021. ISSN 0033-5533. doi: 10.1093/qje/qjaa044. URL https://doi.org/10.1093/qje/qjaa044.

J. Castro-Vincenzi. Climate Hazards and Resilience in the Global Car Industry. 2024.

J. Castro-Vincenzi, G. Khanna, N. Morales, and N. Pandalai-Nayar. Weathering the Storm: Supply Chains and Climate Risk, Mar. 2024. URL https://www.nber.org/papers/w32218.

W. Chen, J. Fan, and W. Luo. Trade and Technology Compatibility in General Equilibrium. *SSRN Electronic Journal*, 2023. ISSN 1556-5068. doi: 10.2139/ssrn.4647210. URL https://www.ssrn.com/abstract=4647210.

D. P. Clark, V. Kozlova, and G. Schaur. Supply Chain Uncertainty in Ocean Transit as a Trade Barrier. 2024.

J.-L. Cruz and E. Rossi-Hansberg. The Economic Geography of Global Warming. *Review of Economic Studies*, 91(2):899–939, Mar. 2024. ISSN 0034-6527, 1467-937X. doi: 10.1093/restud/rdad042. URL https://academic.oup.com/restud/article/91/2/899/7107009.

K. Desmet and E. Rossi-Hansberg. On the spatial economic impact of global warming. *Journal of Urban Economics*, 88:16–37, July 2015. ISSN 00941190. doi: 10.1016/j.jue.2015.04.004. URL https://linkinghub.elsevier.com/retrieve/pii/S0094119015000339.

A. Dube, D. Girardi, Jordà, and A. M. Taylor. A Local Projections Approach to Difference-in-Differences, 2023. URL https://www.nber.org/papers/w31184.

C. Ducruet, R. Juhász, D. K. Nagy, and C. Steinwender. All aboard: The effects of port development. *Journal of International Economics*, 151:103963, Sept. 2024. ISSN 0022-1996. doi: 10.1016/j.jinteco.2024.103963. URL https://www.sciencedirect.com/science/article/pii/S0022199624000904.

P. D. Fajgelbaum and E. Schaal. Optimal Transport Networks in Spatial Equilibrium. *Econometrica*, 88(4):1411–1452, 2020. ISSN 1468-0262. doi: 10.3982/ECTA15213. URL https://onlinelibrary.wiley.com/doi/abs/10.3982/ECTA15213. _eprint: https://onlinelibrary.wiley.com/doi/pdf/10.3982/ECTA15213.

S. Ganapati, W. F. Wong, and O. Ziv. Entrepôt: Hubs, Scale, and Trade Costs. *American Economic Journal: Macroeconomics*, 16(4):239–278, 2024. ISSN 1945-7707. doi: 10.1257/mac.20220250. URL https://www.aeaweb.org/articles?id=10.1257/mac.20220250.

A. Grover and M. E. Kahn. Firm Adaptation to Climate Change, Aug. 2024. URL https://papers.ssrn.com/abstract=4929527.

S. M. Hsiang and A. S. Jina. The Causal Effect of Environmental Catastrophe on Long-Run Economic Growth: Evidence From 6,700 Cyclones, July 2014. URL https://www.nber.org/papers/w20352.

R. Jia, X. Ma, and V. W. Xie. Expecting Floods: Firm Entry, Employment, and Aggregate Implications, July 2022. URL https://www.nber.org/papers/w30250.

K. R. Knapp, M. C. Kruk, D. H. Levinson, H. J. Diamond, and C. J. Neumann. The International Best Track Archive for Climate Stewardship (IBTrACS). Mar. 2010. doi: 10.1175/2009BAMS2755.1. URL https://journals.ametsoc.org/view/journals/bams/91/3/2009bams2755_1.xml. Section: Bulletin of the American Meteorological Society.

A. Martinez. Trade Relationships During and After a Crisis: Evidence from Road Disruptions in Colombian Flower Exports. *Working Paper*, 2024.

S. Nirandjan, E. E. Koks, P. J. Ward, and J. C. J. H. Aerts. A spatially-explicit harmonized global dataset of critical infrastructure. *Scientific Data*, 9(1):150, Apr. 2022. ISSN 2052-4463. doi: 10.1038/s41597-022-01218-4. URL https://www.nature.com/articles/s41597-022-01218-4. Publisher: Nature Publishing Group.

E. Oberfield. A Theory of Input–Output Architecture. *Econometrica*, 86 (2):559–589, 2018. ISSN 1468-0262. doi: 10.3982/ECTA10731. URL https://onlinelibrary.wiley.com/doi/abs/10.3982/ECTA10731. _eprint: https://onlinelibrary.wiley.com/doi/pdf/10.3982/ECTA10731.

N. M. C. Pankratz and C. Schiller. Climate Change and Adaptation in Global Supply-Chain Networks. SSRN Scholarly Paper ID 3475416, Social Science Research Network, Rochester, NY, June 2021. URL https://papers.ssrn.com/abstract=3475416.

A. Rabano and J. N. Rosas. The Transmission of Climate Shocks: The Case of Floods in India. *Working Paper*, 2024.

E. Rossi-Hansberg and J. Zhang. Local GDP Estimates Around the World, Feb. 2025. URL https://www.nber.org/papers/w33458.

I. Rudik, G. Lyn, W. Tan, and A. Ortiz-Bobea. The Economic Effects of Climate Change in Dynamic Spatial Equilibrium, June 2021. URL https://osf.io/usghb_v1.

UNCTAD. Port Industry Survey on Climate Change Impacts and Adaptation. Technical report, Jan. 2018. URL https://unctad.org/system/files/official-document/ser-rp-2017d18_en.pdf.

G. A. Vecchi, C. Landsea, W. Zhang, G. Villarini, and T. Knutson. Changes in Atlantic major hurricane frequency since the late-19th century. *Nature Communications*, 12(1): 4054, July 2021. ISSN 2041-1723. doi: 10.1038/s41467-021-24268-5. URL https://www.nature.com/articles/s41467-021-24268-5. Publisher: Nature Publishing Group.

J. Verschuur, E. E. Koks, and J. W. Hall. Port disruptions due to natural disasters: Insights into port and logistics resilience. *Transportation Research Part D: Transport and Environment*, 85:102393, Aug. 2020. ISSN 1361-9209. doi: 10.1016/j.trd.2020.102393. URL https://www.sciencedirect.com/science/article/pii/S1361920920305800.

J. Verschuur, E. E. Koks, and J. W. Hall. Systemic risks from climate-related disruptions at ports. *Nature Climate Change*, 13(8):804–806, Aug. 2023a. ISSN 1758-6798. doi: 10.1038/s41558-023-01754-w. URL https://www.nature.com/articles/s41558-023-01754-w. Publisher: Nature Publishing Group.

J. Verschuur, E. E. Koks, S. Li, and J. W. Hall. Multi-hazard risk to global port infrastructure and resulting trade and logistics losses. *Communications Earth & Environment*, 4(1):1–12, Jan. 2023b. ISSN 2662-4435. doi: 10.1038/s43247-022-00656-7. URL https://www.nature.com/articles/s43247-022-00656-7. Publisher: Nature Publishing Group.

C. Volpe Martincus and J. Blyde. Shaky roads and trembling exports: Assessing the trade effects of domestic infrastructure using a natural experiment. *Journal of International Economics*, 90(1):148–161, May 2013. ISSN 0022-1996. doi: 10.1016/j.jinteco.2012.11.001. URL https://www.sciencedirect.com/science/article/pii/S0022199612001705.

W. F. Wong and S. Fuchs. Multimodal Transport Networks, Oct. 2022. URL https://papers.ssrn.com/abstract=4277194.

Appendix

A ANECDOTAL EVIDENCE

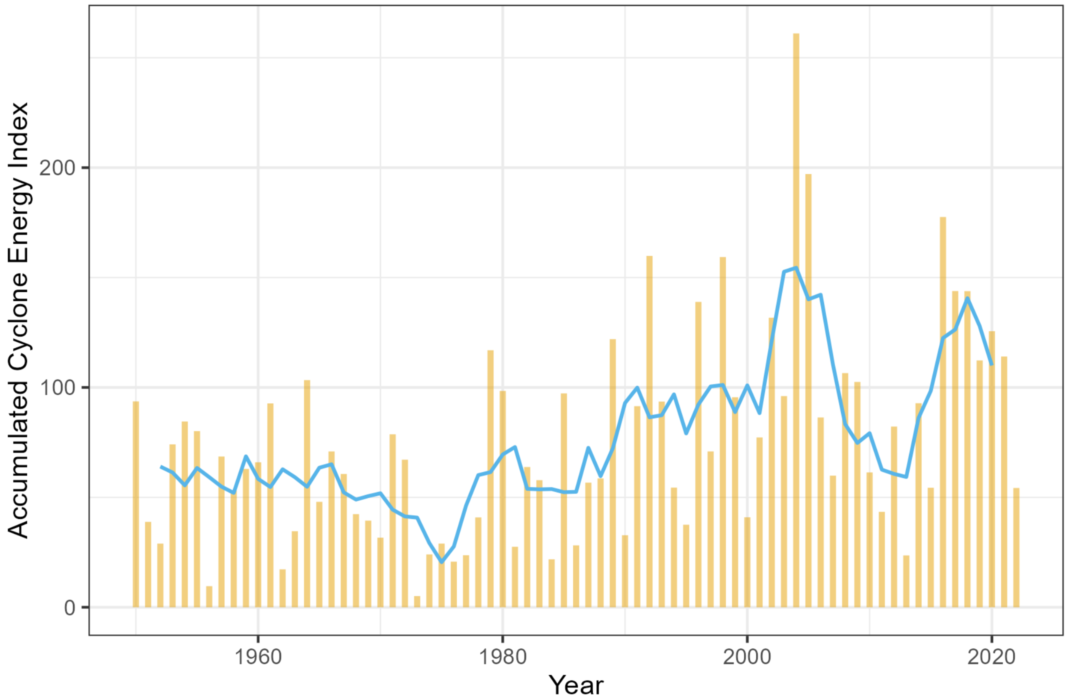

Figure A.1: Annual cyclone activity (ACE) around US shores, 1950-2022

Notes: This figure represents the total annual Accumulated Cyclone Energy (ACE) Index values, a measure of cyclone intensity accounting for cyclone strength, duration, and frequency, within a 200km radius around US shores. The blue line represents a 5-year moving average.

Marine Safety Information Bulletin

Commander
U.S. Coast Guard
Sector Key West
100 Trumbo Road
Key West, FL 33040-6655

MSIB Number: SKW-28-24
Date: Oct 7, 2024
Contact: LT Hailye Wilson
Phone: (305) 292-8768
Email: SKWWaterways@uscg.mil

U.S. COAST GUARD SECTOR KEY WEST PORT CONDITION ZULU

On October 8, 2024, at 0600 (6:00 AM), the Captain of the Port will set Port Condition (PORTCON) **ZULU** for the Port of Key West. The shift is based on the projected arrival of sustained gale force winds (greater than 34 knots/39mph) associated with Hurricane Milton. The table below summarizes COTP requirements for PORTCON Zulu in accordance with 33 CFR 165.707:

Hours Prior to Gales	Port Condition	Requirements *(annotated from 33 CFR 165.707)*
72	Whiskey	• Oceangoing vessels greater than 300 gross tons (GT) must make plans to depart no later than the setting of Port Condition Yankee unless authorized by the COTP. Vessels intending to remain in port must contact the COTP prior to setting PORTCON X-Ray.
48	X-Ray	• Vessels greater than 300 GT without an approval to remain in port must depart prior to the setting of PORTCON Yankee. • All vessels, regulated facilities, and waterfront facilities must ensure that potential flying debris is removed or secured. HAZMAT/pollution hazards must be secured in a safe manner away from waterfront areas.
24	Yankee	• The port is closed to all inbound vessel traffic. All vessels greater than 300 GT must have departed the port, unless authorized by the COTP.
12	Zulu	• The port is closed to all vessel traffic except as specifically authorized by the COTP. • Regulated facilities must cease all cargo operations, including bunkering and lightering.
After Storm's Passage	Four *(All Clear)*	• The port will be re-opened only after satisfactory assessments of the waterways, including critical aids to navigation verifications, have been conducted.

Mariners should be aware that no "safe havens" exist within the Florida Keys for vessels to safely survive hurricane force winds or storm surges without creating a threat to the safety of the port and public welfare. Owners/operators of vessels greater than 300 GT desiring to remain in port throughout hurricane season who have not already submitted heavy weather plans to the COTP for review should be prepared to depart no later than the setting of PORTCON Yankee. *Remain in Port Checklists* are available for review on the Sector Key West HOMEPORT website: https://homeport.uscg.mil/port-directory/key-west. Regulated facilities are reminded to review and update their heavy weather response plans to safely weather any storm that may approach the Florida Keys.

Mariners navigating through the Islamorada Snake Creek Draw Bridge are reminded that the bridge may not operate on normally published schedules as early as 36 hours prior to forecasted storm's arrival. The bridge will not open for maritime traffic upon arrival of gale force winds (34 knots or higher) or following a mandatory Monroe County evacuation order.

The official PORTCON and associated Marine Safety Information Bulletin (MSIB) will be set on Sector Key West's Homeport website. As weather conditions may change rapidly, mariners are encouraged to monitor the National Weather Service's forecasts and observations at https://www.weather.gov/key or on NOAA weather radios. For questions or additional information, call Coast Guard Sector Key West at (305) 292-8727 or email SKW@uscg.mil.

Sincerely,

J. D. INGRAM
Captain, U. S. Coast Guard
Captain of the Port

This Marine Safety Information Bulletin has been issued for public information and notification purposes.

Figure A.2: Example of port condition ZULU

Notes: This document is the Marine Safety Information Bulletin issued on October 8, 2024, by the US Coast Guards of Port Key West (Florida), before the landfall of Hurricane Milton.

B DATA

B.1 BILL OF LADING DATA — BRAZIL

Table B.1: Data Cleaning - Firms and Relationships

	Desc.	Num. Shipments	Num. Importers	Num. Exporters	Num. Rel.
Relationship Sample					
(1)	Raw Panjiva	5658662	37657	28042	134524
(2)	Drop missing parent company ID	5621336	37628	28006	134294
(3)	Drop poorly geolocalized firms	1432748	22285	22926	87687
(4)	Drop poorly reported ports	1431912	22284	22916	87630
(5)	Keep Brazilian imp., foreign exp.	1427963	22107	22534	86847
(6)	Drop NVO/forwarders	574010	13500	16189	45690
(7)	Drop infrequent rel.	545259	7853	9105	23020
Relationship-Route Sample					
(8)	Only treated relationships	120096	1084	556	1906

Note: This table reports the effect of the data cleaning procedure on firm-related variables. Firms refer to geolocalized establishments. "Num. Shipments" refers to the number of distinct shipments, as identified by the bill of lading ID. "Num. Importers" refers to the number of establishments importing goods. "Num. Exporters" refers to the number of establishments exporting goods. "Num. Rel." refers to the number of trading establishment pairs.

Table B.2: Data Cleaning - Maritime Ports and Routes

	Desc.	Num. Exit Ports	Num. Entry Ports	Num. Routes	Num. Rel.-Routes
Relationship Sample					
(1)	Raw Panjiva	773	48	4081	392635
(2)	Drop missing parent company ID	765	48	4029	390428
(3)	Drop poorly geolocalized firms	363	41	1500	160648
(4)	Drop poorly reported ports	359	40	1477	160308
(5)	Keep Brazilian imp., foreign exp.	353	40	1461	159261
(6)	Drop NVO/forwarders	329	39	1352	71423
(7)	Drop infrequent rel.	268	34	1088	48402
Relationship-Route Sample					
(8)	Only treated relationships	85	30	384	5735

Note: This table reports the effect of the data cleaning procedure on route-related variables. Routes refer to port of exit-port of entry pairs. "Num. Exit Ports" refers to the number of port of lading, as identified by the UN/LOCODE. "Num. Entry Ports" refers to the number of port of unlading, as identified by UN/LOCODE. "Num. Routes" refers to the number of observed port pairs. "Num. Rel.Routes" refers to the number of importer-exporter-route triplets.

Table B.3: Summary Statistics - Relationship Sample

Desc.	Mean	25%	50%	75%	90%	95%
Per Buyer - Month						
Num. transactions	5.88	1.00	2.00	4.00	10.00	18.00
Num. suppliers	1.64	1.00	1.00	2.00	3.00	4.00
Num. exit ports	1.65	1.00	1.00	2.00	3.00	4.00
Num. entry ports	1.10	1.00	1.00	1.00	1.00	2.00
Num. routes	1.69	1.00	1.00	2.00	3.00	4.00
Log weight (kg)	10.87	9.86	10.68	11.85	13.05	13.89
Log volume (TEU)	1.49	0.69	1.39	2.30	3.40	4.09
Log value (USD)	11.93	10.89	11.77	12.85	13.95	14.72
Per Supplier - Month						
Num. transactions	5.74	1.00	2.00	4.00	9.00	17.00
Num. buyers	1.60	1.00	1.00	1.00	2.00	4.00
Num. exit ports	1.32	1.00	1.00	1.00	2.00	3.00
Num. entry ports	1.26	1.00	1.00	1.00	2.00	2.00
Num. routes	1.52	1.00	1.00	1.00	2.00	3.00
Log weight (kg)	10.57	9.63	10.42	11.59	12.80	13.65
Log volume (TEU)	1.37	0.69	1.10	2.20	3.26	3.95
Log value (USD)	11.94	10.90	11.80	12.90	14.05	14.85
Per Relationship - Month						
Num. transactions	3.59	1.00	1.00	2.00	5.00	10.00
Num. exit ports	1.15	1.00	1.00	1.00	2.00	2.00
Num. entry ports	1.03	1.00	1.00	1.00	1.00	1.00
Num. routes	1.17	1.00	1.00	1.00	2.00	2.00
Log weight (kg)	10.44	9.67	10.20	11.34	12.42	13.17
Log volume (TEU)	1.16	0.00	0.69	1.79	2.89	3.50
Log value (USD)	11.64	10.73	11.51	12.47	13.49	14.21

Note: The table reports summary statistics of the relationship sample. "Num. Shipments" refers to the number of distinct shipments, as identified by the bill of lading ID. "Num. exit ports" refers to the number of ports of exit, as identified by the UN/LOCODE. "Num. entry ports" refers to the number of ports of entry, as identified by the UN/LOCODE. "Num. routes" refers to the number of pairs or ports of exit and entry. "Log weight (kg)" refers to the total weight of shipments, in kilograms. "Log volume (TEU)" refers to the total volume of shipments, in Twenty-foot Equivalent Units. "Log value (USD)" refers to the total value of shipments, in current USD.

Table B.4: Summary Statistics - Relationship-Route Sample

Desc.	Mean	25%	50%	75%	90%	95%
Per Buyer - Month						
Num. shipments	7.73	1.00	2.00	6.00	18.00	37.00
Num. suppliers	1.26	1.00	1.00	1.00	2.00	3.00
Num. exit ports	1.76	1.00	1.00	2.00	3.00	5.00
Num. entry ports	1.11	1.00	1.00	1.00	1.00	2.00
Num. routes	1.81	1.00	1.00	2.00	4.00	5.00
Log weight (kg)	11.13	9.88	10.88	12.14	13.51	14.43
Log volume (TEU)	1.81	0.69	1.61	2.77	3.89	4.62
Log value (USD)	11.97	10.79	11.72	12.96	14.22	15.03
Per Supplier - Month						
Num. shipments	12.67	1.00	3.00	10.00	30.00	58.00
Num. buyers	2.07	1.00	1.00	2.00	3.00	6.00
Num. exit ports	1.99	1.00	1.00	2.00	4.00	6.00
Num. entry ports	1.39	1.00	1.00	1.00	2.00	3.00
Num. routes	2.38	1.00	1.00	2.00	5.00	7.00
Log weight (kg)	11.22	9.82	11.04	12.37	13.76	14.69
Log volume (TEU)	2.09	0.69	1.95	3.09	4.29	4.99
Log value (USD)	12.35	11.02	12.18	13.48	14.82	15.73
Per Relationship - Month						
Num. shipments	6.11	1.00	2.00	5.00	13.00	28.00
Num. exit ports	1.50	1.00	1.00	1.00	3.00	4.00
Num. entry ports	1.07	1.00	1.00	1.00	1.00	2.00
Num. routes	1.54	1.00	1.00	2.00	3.00	4.00
Log weight (kg)	10.90	9.78	10.65	11.87	13.15	14.09
Log volume (TEU)	1.62	0.69	1.39	2.48	3.61	4.29
Log value (USD)	11.81	10.71	11.56	12.73	13.93	14.76

Note: The table reports summary statistics of the relationship-route sample. It contains only treated relationships. "Num. Shipments" refers to the number of distinct shipments, as identified by the bill of lading ID. "Num. exit ports" refers to the number of ports of exit, as identified by the UN/LOCODE. "Num. entry ports" refers to the number of ports of entry, as identified by the UN/LOCODE. "Num. routes" refers to the number of pairs or ports of exit and entry. "Log weight (kg)" refers to the total weight of shipments, in kilograms. "Log volume (TEU)" refers to the total volume of shipments, in Twenty-foot Equivalent Units. "Log value (USD)" refers to the total value of shipments, in current USD.

B.2 BILL OF LADING DATA — US

Table B.5: Summary Statistics - U.S. Ports Exporting to Brazil (per day)

Desc.	Mean	10%	25%	50%	75%	90%
Num. vessels	4.60	1.00	2.00	3.00	7.00	10.00
Num. shipments	214.47	2.00	4.00	56.00	323.00	652.00
Num. exporters	89.09	1.00	2.00	27.00	148.00	272.00
Log volume (TEU)	6.53	4.70	5.72	6.72	7.61	8.13
Log value (USD)	16.76	14.65	15.87	16.95	17.82	18.93

Note:

B.3 TROPICAL CYCLONES - US

Table B.6: Summary Statistics - Tropical Cyclones

Desc.	Mean	10%	25%	50%	75%	90%
Per Cyclone Event						
Num. ports of lading	4.65	1.00	3.50	5.00	5.50	8.00
Wind speed (knots)	50.34	37.51	40.59	48.07	55.98	68.58
Exposure - 34 knots (hours)	14.85	5.09	7.51	10.05	23.95	28.54
Days to landfall	2.42	1.00	1.00	2.00	3.00	5.00
Per Port - Year						
Num. cyclones	1.44	1.00	1.00	1.00	2.00	2.00
Wind speed (knots)	53.31	37.70	41.57	48.95	60.65	71.84
Exposure - 34 knots (hours)	16.66	4.40	7.43	12.62	19.80	33.83
Days to landfall	2.54	1.00	1.73	3.00	3.00	4.00

Note:

B.4 TROPICAL CYCLONES - PRESENT AND FUTURE CLIMATES (STORM MODEL)

Figure B.1: Present and future (RCP8.5) tropical cyclone climates

(a) Present-day (1980-2015)

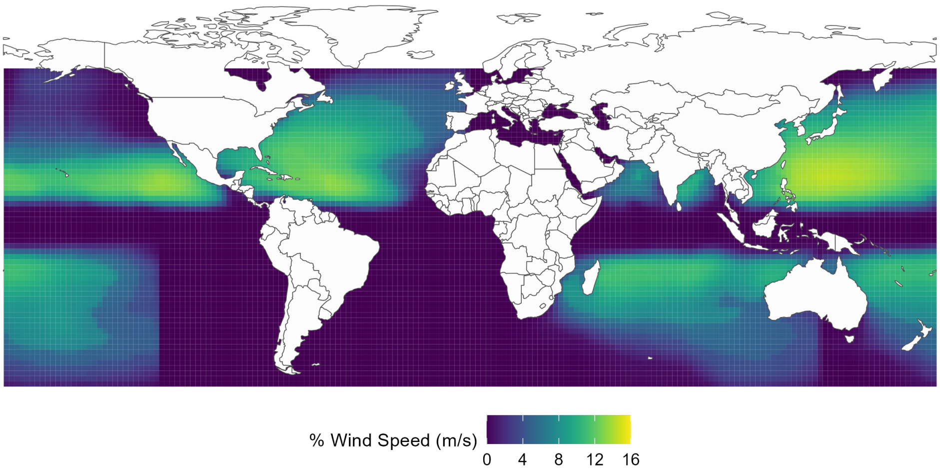

(b) RCP8.5 (2015-2050)

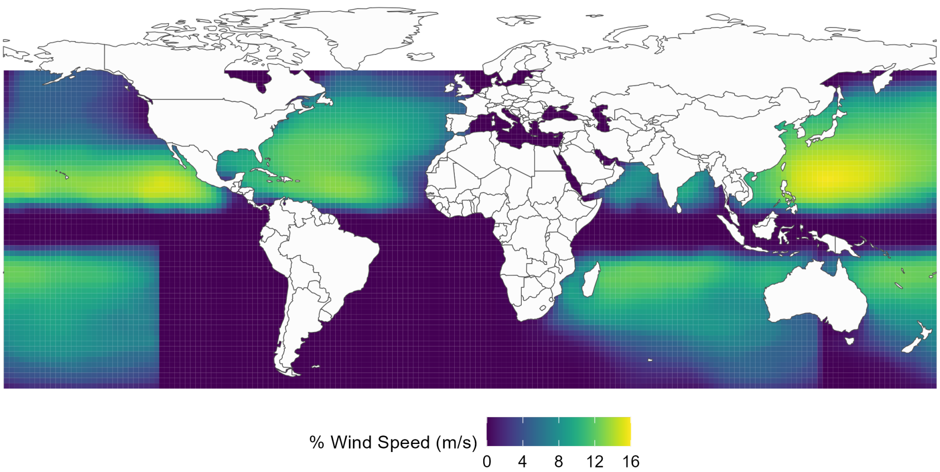

Notes: This map reports expected wind speeds (m/s) induced by tropical cyclones, in the present-day (panel a) and the future RCP8.5 scenario (panel b) of the STORM model.

C Robustness and alternative specifications.

C.1 Additional outcomes.

Figure C.1: Port exposure to cyclones and firm-to-firm relationship (intensive margin)

(a) Log number of shipments (b) Log weight (kg) (c) Log volume (TEU)

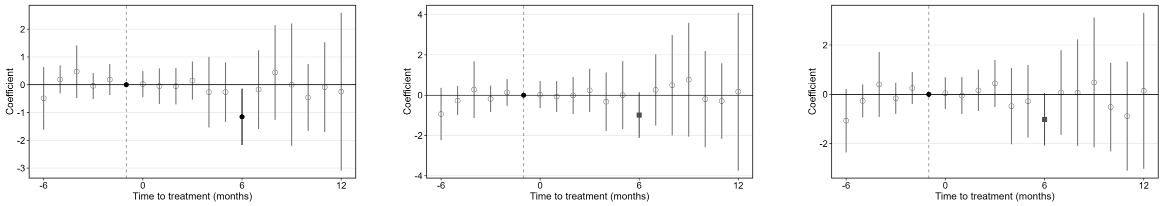

Notes: These panels plot the effect of port exposure to tropical cyclones on firm-to-firm-level outcomes, as specified by Equation (2). The outcome of the left panel (a) is the log number of shipments, conditioned on a positive relationship activity. The outcome of the center panel (b) is the log total weight of shipments in kilograms, conditioned on a positive relationship activity. The outcome of the right panel (c) is the log total volume of shipments in TEU, conditioned on a positive relationship activity. Regressions include buyer-time and supplier-time fixed effects. Standard errors are clustered at the buyer level. The bars correspond to 95% confidence intervals. Black dots are point estimates significant at the 5% level, gray squares are point estimates significant at the 10% level, and empty dots are point estimates non-significant at the 10% level.

C.2 ALTERNATIVE WIND THRESHOLD.

Figure C.2: Port exposure to cyclones and firm-to-firm relationship

(a) Relationship activity (34 knots)

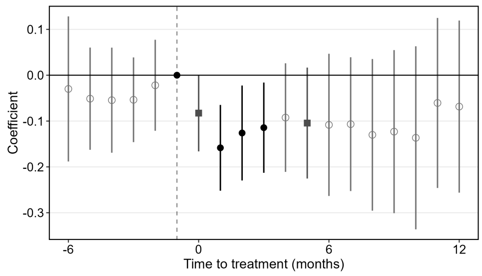

(b) Relationship termination (34 knots)

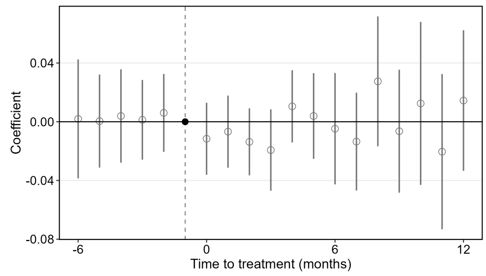

(c) Relationship activity (41 knots)

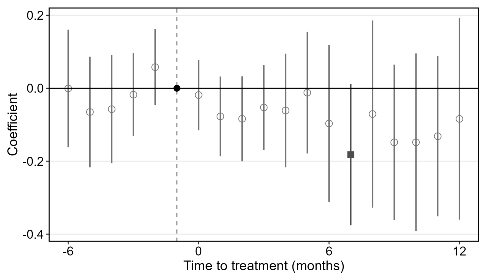

(d) Relationship termination (41 knots)

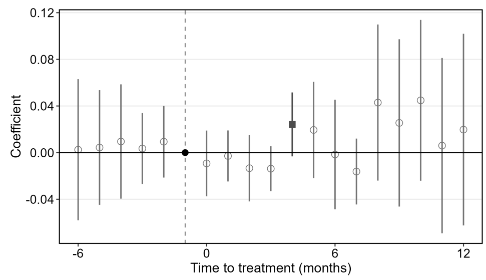

Notes: These panels plot the effect of port exposure to tropical cyclones on firm-to-firm-level outcomes, as specified by Equation (2). The wind threshold for the shock definition is 34 knots for panels (a) and (b), and 41 knots for panels (c) and (d). The outcome of the left panels (a) and (c) is a binary variable, taking value 1 if at least one shipment is observed for the trading pair at month *t* (active relationship), 0 otherwise. Relationship activity is conditioned on the entry and exit of the relationship. The outcome of right panels (b) and (d) is a binary variable, taking value 1 if an observed shipment at month *t* is the last observable shipment of the trading pair (relationship termination), and 0 otherwise. Relationship termination is conditioned on the entry and exit of the relationship. Regressions include buyer-time and supplier-time fixed effects. Standard errors are clustered at the buyer level. The bars correspond to 95% confidence intervals. Black dots are point estimates significant at the 5% level, gray squares are point estimates significant at the 10% level, and empty dots are point estimates non-significant at the 10% level.

Figure C.3: The impact of port exposure to cyclones on route choice

(a) Route activity (34 knots)

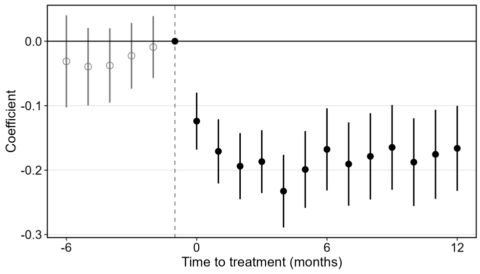

(b) Log share of shipments (34 knots)

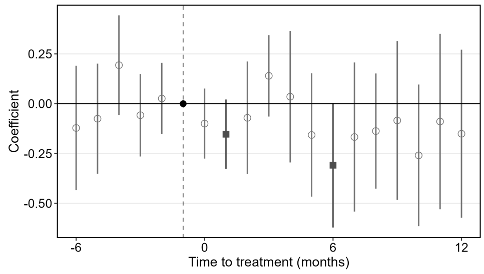

(c) Route activity (41 knots)

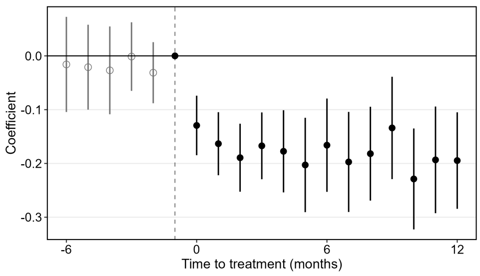

(d) Log share of shipments (41 knots)

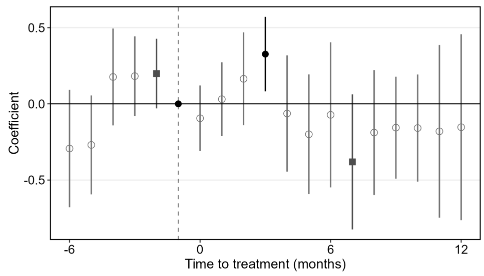

Notes: These panels plot the effect of port exposure to tropical cyclones on firm-to-firm-route-level outcomes, as specified by Equation (3). The wind threshold for the shock definition is 34 knots for panels (a) and (b), and 41 knots for panels (c) and (d). The outcome of the left panels (a) and (c) is a binary variable, taking value 1 if at least one shipment is observed for the trading pair through route *r* at month *t* (active route), 0 otherwise. Route activity is conditioned on the activity of the firm-to-firm relationship. The outcome of the right panels (b) and (d) is the log share of shipments of the relationship, using route *r*. The log share of shipments is conditioned on the activity of the route. Regressions include relationship-time, and port of destination-time fixed effects. Standard errors are clustered at the relationship level. The bars correspond to 95% confidence intervals. Black dots are point estimates significant at the 5% level, gray squares are point estimates significant at the 10% level, and empty dots are point estimates non-significant at the 10% level.

C.3 Alternative exposure thresholds

Figure C.4: Port exposure to cyclones and firm-to-firm relationships

(a) Route activity (12 months exposure)

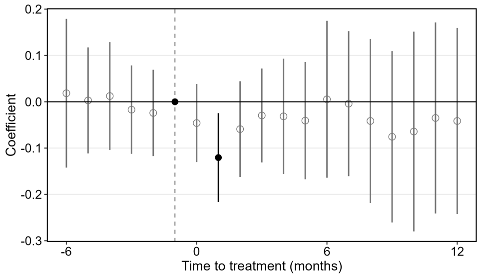

(b) Log share of shipments (12 months)

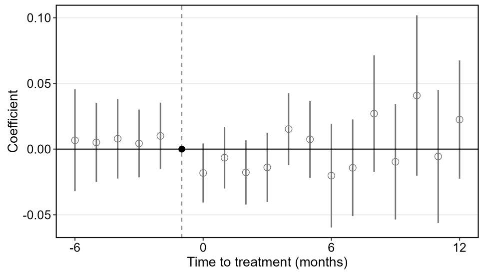

(c) Route activity (24 months)

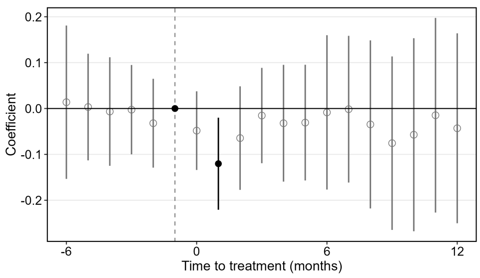

(d) Log share of shipments (24 months)

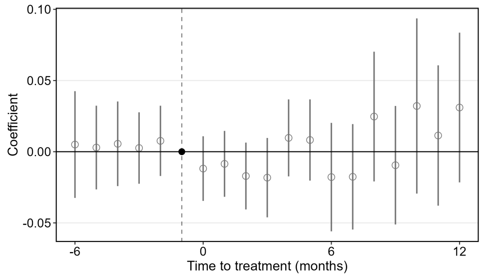

(e) Route activity (All months)

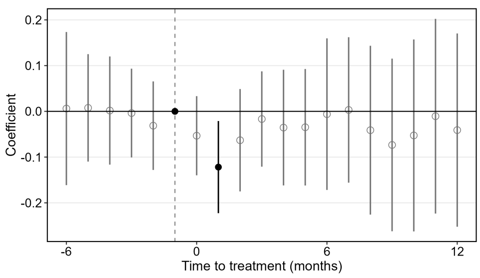

(f) Log share of shipments (All months)

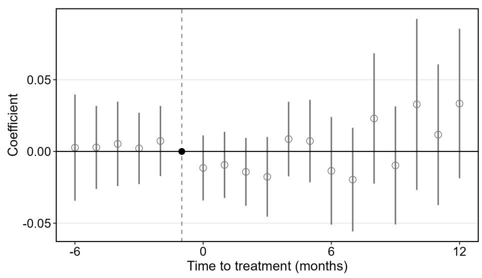

Notes: These panels plot the effect of port exposure to tropical cyclones on firm-to-firm-level outcomes, as specified by Equation (2). The exposure window for the shock definition is 12 months knots for panels (a) and (b), and 24 months for panels (c) and (d), and all months for panel (e) and (f). The outcome of the left panels (a), (c) and (e) is a binary variable, taking value 1 if at least one shipment is observed for the trading pair at month t (active relationship), 0 otherwise. Relationship activity is conditioned on the entry and exit of the relationship. The outcome of right panels (b), (d) and (f) is a binary variable, taking value 1 if an observed shipment at month t is the last observable shipment of the trading pair (relationship termination), and 0 otherwise. Relationship termination is conditioned on the entry and exit of the relationship. Regressions include buyer-time and supplier-time fixed effects. Standard errors are clustered at the buyer level. The bars correspond to 95% confidence intervals. Black dots are point estimates significant at the 5% level, gray squares are point estimates significant at the 10% level, and empty dots are point estimates non-significant at the 10% level.

Figure C.5: The impact of port exposure to cyclones on route choice

(a) Route activity (12 months exposure)

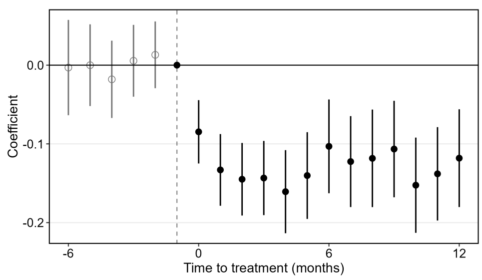

(b) Log share of shipments (12 months)

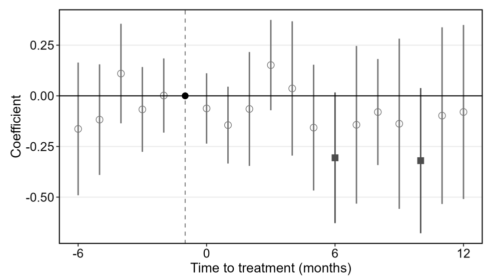

(c) Route activity (24 months)

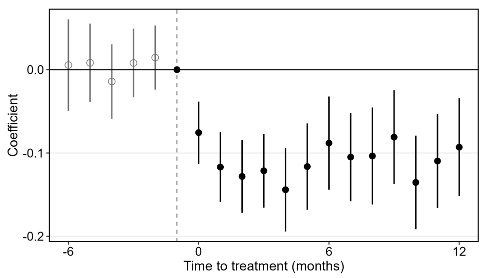

(d) Log share of shipments (24 months)

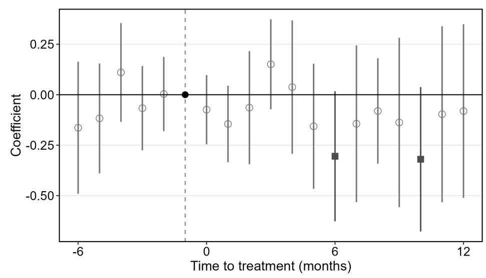

(e) Route activity (All months)

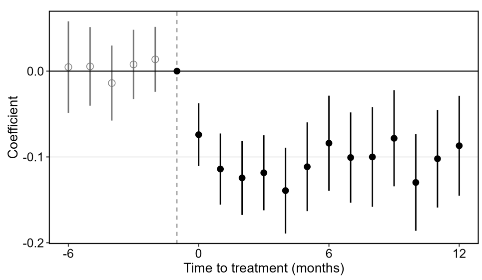

(f) Log share of shipments (All months)

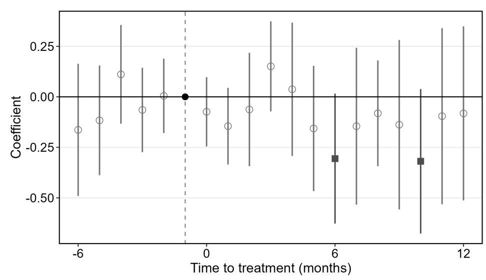

Notes: These panels plot the effect of port exposure to tropical cyclones on firm-to-firm-route-level outcomes, as specified by Equation (3). The exposure window for the shock definition is 12 months knots for panels (a) and (b), and 24 months for panels (c) and (d), and all months for panel (e) and (f). The outcome of the left panels (a), (c), and (e) is a binary variable, taking value 1 if at least one shipment is observed for the trading pair through route *r* at month *t* (active route), 0 otherwise. Route activity is conditioned on the activity of the firm-to-firm relationship. The outcome of the right panels (b), (d) and (f) is the log share of shipments of the relationship, using route *r*. The log share of shipments is conditioned on the activity of the route. Regressions include relationship-time, and port of destination-time fixed effects. Standard errors are clustered at the relationship level. The bars correspond to 95% confidence intervals. Black dots are point estimates significant at the 5% level, gray squares are point estimates significant at the 10% level, and empty dots are point estimates non-significant at the 10% level.

C.4 Absorbing treatments

Figure C.6: Port exposure to cyclones and firm-to-firm relationship

(a) Relationship activity (b) Relationship termination

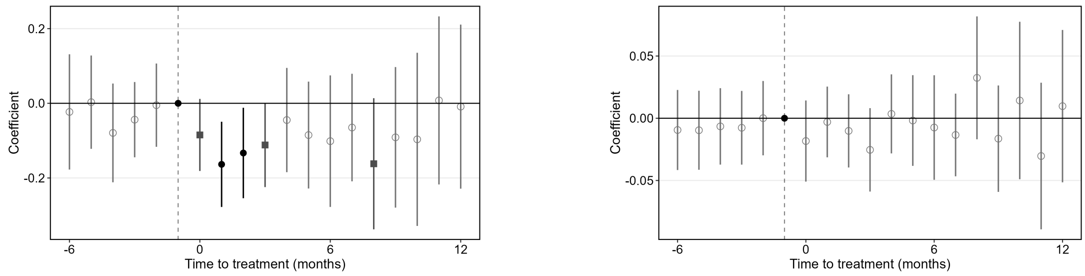

Notes: These panels plot the effect of port exposure to tropical cyclones on firm-to-firm-level outcomes, as specified by Equation (2), but under the assumption of absorbing treatment. The outcome of the left panel (a) is a binary variable, taking value 1 if at least one shipment is observed for the trading pair at month t (active relationship), 0 otherwise. Relationship activity is conditioned on the entry and exit of the relationship. The outcome of right panel (b) is a binary variable, taking value 1 if an observed shipment at month t is the last observable shipment of the trading pair (relationship termination), and 0 otherwise. Relationship termination is conditioned on the entry and exit of the relationship. Regressions include buyer-time and supplier-time fixed effects. Standard errors are clustered at the buyer level. The bars correspond to 95% confidence intervals. Black dots are point estimates significant at the 5% level, gray squares are point estimates significant at the 10% level, and empty dots are point estimates non-significant at the 10% level.

Figure C.7: The impact of port exposure to cyclones on route choice

(a) Route activity (b) Log share of shipments

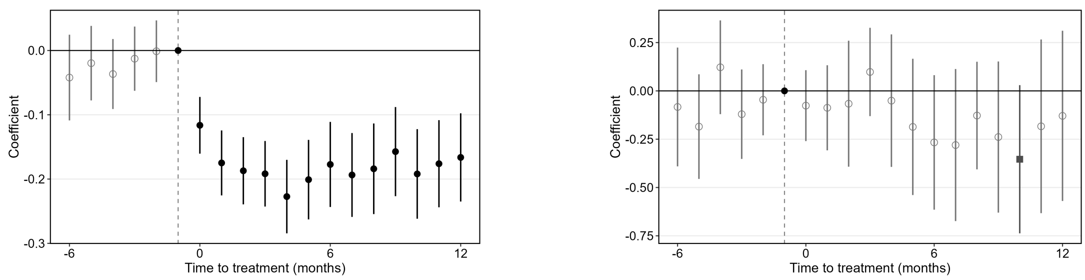

Notes: These panels plot the effect of port exposure to tropical cyclones on firm-to-firm-route-level outcomes, as specified by Equation (3), but under the assumption of absorbing treatments. The outcome of the left panel (a) is a binary variable, taking value 1 if at least one shipment is observed for the trading pair through route r at month t (active route), 0 otherwise. Route activity is conditioned on the activity of the firm-to-firm relationship. The outcome of the right panel (b) is the log share of shipments of the relationship, using route r. The log share of shipments is conditioned on the activity of the route. Regressions include relationship-time, and port of destination-time fixed effects. Standard errors are clustered at the relationship level. The bars correspond to 95% confidence intervals. Black dots are point estimates significant at the 5% level, gray squares are point estimates significant at the 10% level, and empty dots are point estimates non-significant at the 10% level.

D Theory

D.1 Proofs

Proof: Proposition 1. Denote by $\lambda_j(\phi, r) = \frac{c_j}{z(\phi)} \prod_{k=1}^{|\mathcal{B}_r|} d_{r_{k-1},r_k} \prod_{m=1}^{|\mathcal{P}_r|} t_{p(r)_m}$ the *effective* costs of using input from supplier j in technique ϕ, along route r. Consider the probability that the effective cost of supplier $j \in M_{n'}$ available to $i \in M_n$ through route r is strictly lower than a threshold λ,

$$P(\lambda_j(\phi, r) \leq \lambda) = P\left(\frac{c_j}{z(\phi)} \prod_{k=1}^{|\mathcal{B}_r|} d_{r_{k-1},r_k} \prod_{m=1}^{|\mathcal{P}_r|} t_{p(r)_m} \leq \lambda \right) = F_r(\lambda).$$

Integrating F_r over realizations of z and $t_{p(r)_1}, \cdots, t_{p(r)_M}$, we obtain that the number of potential suppliers that deliver effective cost weakly less than λ through route r follows a Poisson distribution with mean

$$\begin{aligned}
\Lambda_{jr} &= \int_0^\infty \left[\int_1^\infty \cdots \int_1^\infty F_r(\lambda) dF_{p(r)_1}(t) \cdots dF_{p(r)_M}(t) \right] dF_r(z) \\
&= \int_0^\infty \left[\int_1^\infty \cdots \int_1^\infty \left[\int_0^\infty \mathbb{1}\left(\frac{c_j}{z(\phi)} \prod_{k=1}^{|\mathcal{B}_r|} d_{r_{k-1},r_k} \prod_{m=1}^{|\mathcal{P}_r|} t_{p(r)_m} \leq \lambda \right) dF_{n'}(c_j) \right] dF_{p(r)_1}(t) \cdots dF_{p(r)_M}(t) \right] \xi a_{n'} z \\
&= a_{n'} \lambda^\xi \prod_{k=1}^{|\mathcal{B}_r|} d_{r_{k-1},r_k}^{-\xi} \int_0^\infty \left[\int_1^\infty \cdots \int_1^\infty \left[\int_0^\infty \mathbb{1}\left(c_j \leq u \right) dF_{n'}(c_j) \right] \prod_{m=1}^{|\mathcal{P}_r|} t_{p(r)_m}^{-\xi} dF_{p(r)_1}(t) \cdots dF_{p(r)_M}(t) \right] \xi u^{-\xi} \\
&= a_{n'} \lambda^\xi \prod_{k=1}^{|\mathcal{B}_r|} d_{r_{k-1},r_k}^{-\xi} \left[\int_1^\infty \int_1^\infty \cdots \int_1^\infty \left[\int_0^\infty c_j^{-\xi} dF_{n'}(c_j) \right] \prod_{m=1}^{|\mathcal{P}_r|} t_{p(r)_m}^{-\xi} dF_{p(r)_1}(t) \cdots dF_{p(r)_M}(t) \right] \xi s^{-\xi-1} ds \\
&= a_{n'} \lambda^\xi \bar{c}_j^{-\xi} \prod_{k=1}^{|\mathcal{B}_r|} d_{r_{k-1},r_k}^{-\xi} \prod_{m=1}^{|\mathcal{P}_r|} \bar{t}_{p(r)_m}^{-\xi},
\end{aligned} \tag{21}$$

where

$$\bar{c}_j^{-\xi} = \int_0^\infty c_j^{-\xi} dF_{n'}(c_j) \quad \text{and} \quad \bar{t}_{p(r)_m}^{-\xi} = \int_1^\infty t_{p(r)_m}^{-\xi} dF_{p(r)_m}(t) \tag{22}$$

The second equality follows when applying the transformation $z\lambda / \left(\prod_{k=1}^{|\mathcal{B}_r|} d_{r_{k-1},r_k} \prod_{m=1}^{|\mathcal{P}_r|} t_{p(r)_m} \right) = u$, while the third equality follows when applying the transformation $u/c_j = s$. Therefore, number of potential suppliers along route r that deliver effective cost strictly greater than λ is such that:

$$P(\lambda_j(\phi, r) > \lambda) = e^{-\Lambda_{jr}} = e^{-a_{n'} \lambda^\xi \bar{c}_j^{-\xi} \prod_{k=1}^{|\mathcal{B}_r|} d_{r_{k-1},r_k}^{-\xi} \prod_{m=1}^{|\mathcal{P}_r|} \bar{t}_{p(r)_m}^{-\xi}}. \tag{23}$$

Consider now the cost distribution of firm $i \in M_n$ with a supplier $j \in M_{n'}$ along route r. Using the marginal cost of firm i, one obtains

$$\begin{aligned} P\left(c_i(\phi,r) > c\right) &= P\left(\frac{w_n^{1-\alpha}}{a_n}\left(\tau_{n(i)n(j)}(r)\frac{c_j}{z(\phi)}\right)^{\alpha} > c\right) \\ &= P\left(\lambda_j(\phi,r) > \left(a_n w_n^{\alpha-1} c\right)^{\frac{1}{\alpha}}\right) \\ &= exp\left[-\left(a_{n'} c^{\frac{\xi}{\alpha}}\left(a_n w_n^{\alpha-1}\right)^{\frac{\xi}{\alpha}} \prod_{k=1}^{|\mathcal{B}_r|} d_{r_{k-1},r_k}^{-\xi} \prod_{m=1}^{|\mathcal{P}_r|} \bar{t}_{p(r)_m}^{-\xi} \bar{c}_j^{-\xi}\right)\right]. \end{aligned} \tag{24}$$

Then the probability that firm i's minimal cost from sourcing from n' through route r is higher than a threshold, $P\left(c_i(\phi,r)_{\min,r} > c\right)$ is as follows:

$$\begin{aligned} P\left(c_i(\phi,r)_{\min,r} > c\right) &= P\left(\lambda_j(\phi,r)_{\min,r} > \left(a_n w_n^{\alpha-1} c\right)^{\frac{1}{\alpha}}\right) \\ &= exp\left[-a_{n'} c^{\frac{\xi}{\alpha}}\left(a_n w_n^{\alpha-1}\right)^{\frac{\xi}{\alpha}} \prod_{k=1}^{|\mathcal{B}_r|} d_{r_{k-1},r_k}^{-\xi} \prod_{m=1}^{|\mathcal{P}_r|} \bar{t}_{p(r)_m}^{-\xi} \bar{c}_{n'}^{-\xi}\right]. \end{aligned} \tag{25}$$

Consider finally the minimum cost at which firm i can produce (sourcing from any supplier through any route $r \in \mathcal{R}$), given realizations of a_n:

$$\begin{aligned} P(c_i(\phi,r)_{\min,r\in\mathcal{R}} > c) &= \prod_{r\in\mathcal{R}} P\left(c_i(\phi,r)_{\min,r} > c\right) \\ &= \prod_{r\in\mathcal{R}} exp\left[-a_{n'} c^{\frac{\xi}{\alpha}}\left(a_n w_n^{\alpha-1}\right)^{\frac{\xi}{\alpha}} \prod_{k=1}^{|\mathcal{B}_r|} d_{r_{k-1},r_k}^{-\xi} \prod_{m=1}^{|\mathcal{P}_r|} \bar{t}_{p(r)_m}^{-\xi} \bar{c}_{n'}^{-\xi}\right] \\ &= exp\left[-\left(a_n w_n^{\alpha-1}\right)^{\frac{\xi}{\alpha}}\left(\sum_{n'} a_{n'} \bar{c}_{n'}^{-\xi} \sum_{r\in\mathcal{R}_{n'n}} \prod_{k=1}^{|\mathcal{B}_r|} d_{r_{k-1},r_k}^{-\xi} \prod_{m=1}^{|\mathcal{P}_r|} \bar{t}_{p(r)_m}^{-\xi}\right) c^{\frac{\xi}{\alpha}}\right]. \end{aligned} \tag{26}$$

which is Weibull distributed. It remains to characterize $\bar{c}_n$ and $\bar{\theta}_r$, both moments of the respective marginal cost and trade cost distributions. Consider first

$$\begin{aligned}
\bar{c}_n^{-\xi} &= \int_0^\infty c^{-\xi} d\left\{1 - exp\left[-\left(a_n w_n^{\alpha-1}\right)^{\frac{\xi}{\alpha}}\left(\sum_{n'} a_{n'}\bar{c}_{n'}^{-\xi}\sum_{r\in\mathcal{R}_{n'n}}\prod_{k=1}^{|\mathcal{B}_r|} d_{r_{k-1},r_k}^{-\xi}\prod_{m=1}^{|\mathcal{P}_r|}\bar{t}_{p(r)_m}^{-\xi}\right) c^{\frac{\xi}{\alpha}}\right]\right\} \\
&= a_n^{\xi} w_n^{(\alpha-1)\xi}\left(\sum_{n'} a_{n'}\bar{c}_{n'}^{-\xi}\sum_{r\in\mathcal{R}_{n'n}}\prod_{k=1}^{|\mathcal{B}_r|} d_{r_{k-1},r_k}^{-\xi}\prod_{m=1}^{|\mathcal{P}_r|}\bar{t}_{p(r)_m}^{-\xi}\right)^{\alpha}\int_0^\infty u^{-\xi} d\left\{1 - exp\left[-u^{\frac{\xi}{\alpha}}\right]\right\} \\
&= a_n^{\xi} w_n^{(\alpha-1)\xi}\left(\sum_{n'} a_{n'}\bar{c}_{n'}^{-\xi}\sum_{r\in R_{nn'}}\prod_{k=1}^{|\mathcal{B}_r|} d_{r_{k-1},r_k}^{-\xi}\prod_{m=1}^{|\mathcal{P}_r|}\bar{t}_{p(r)_m}^{-\xi}\right)^{\alpha}\int_0^\infty v^{-\alpha} d\left\{1 - e^{-v}\right\} \\
&= a_n^{\xi} w_n^{(\alpha-1)\xi}\left(\sum_{n'} a_{n'}\bar{c}_{n'}^{-\xi}\sum_{r\in\mathcal{R}_{n'n}}\prod_{k=1}^{|\mathcal{B}_r|} d_{r_{k-1},r_k}^{-\xi}\prod_{m=1}^{|\mathcal{P}_r|}\bar{t}_{p(r)_m}^{-\xi}\right)^{\alpha}\int_0^\infty v^{-\alpha} e^{-v} dv \\
&= a_n^{\xi} w_n^{(\alpha-1)\xi}\left(\sum_{n'} a_{n'}\bar{c}_{n'}^{-\xi}\sum_{r\in\mathcal{R}_{n'n}}\prod_{k=1}^{|\mathcal{B}_r|} d_{r_{k-1},r_k}^{-\xi}\prod_{m=1}^{|\mathcal{P}_r|}\bar{t}_{p(r)_m}^{-\xi}\right)^{\alpha}\Gamma(1-\alpha).
\end{aligned} \tag{27}$$

The second equality follows from applying the transformation

$$a_n w_n^{\alpha-1}\left(\sum_{n'} a_{n'}\bar{c}_{n'}^{-\xi}\sum_{r\in\mathcal{R}_{n'n}}\prod_{k=1}^{|\mathcal{B}_r|} d_{r_{k-1},r_k}^{-\xi}\prod_{m=1}^{|\mathcal{P}_r|}\bar{t}_{p(r)_m}^{-\xi}\right)^{\frac{\alpha}{\xi}} c = u.$$

The third equality follows from applying the transformation $v = u^{\frac{\xi}{\alpha}}$.

Moreover, $\bar{t}_{p(r)_m}^{-\xi}$ follows immediately from its definition and the Pareto assumptions on its distribution:

$$\begin{aligned}
\bar{t}_{p(r)_m}^{-\xi} &= \int_1^\infty t_{p(r)_m}^{-\xi} dF_{p(r)_m}(t) \\
&= \int_1^\infty t_{p(r)_m}^{-\xi} d\{1 - t^{-\psi_{p(r)_m}}\} \\
&= \frac{\psi_{p(r)_m}}{\psi_{p(r)_m} + \xi}.
\end{aligned} \tag{28}$$

Proof: Corollary 1. From the cost distribution of firm $i \in M_{n'}$ sourcing from route r, the number of suppliers located in n and using route r available to firm i in city n', such that i achieves a cost below c is distributed Poisson with parameter

$$\rho_{i,r} = a_n c^{\frac{\xi}{\alpha}} \left(a_{n'} w_{n'}^{\alpha-1}\right)^{\frac{\xi}{\alpha}} \prod_{k=1}^{|\mathcal{B}_r|} d_{r_{k-1},r_k}^{-\xi} \prod_{m=1}^{|\mathcal{P}_r|} \bar{t}_{p(r)_m}^{-\xi} \bar{c}_n^{-\xi}. \tag{29}$$

Moreover, from the cost distribution of firm $i \in M_{n'}$ sourcing from any route, the number of suppliers available to firm i from any route, such that i achieves a cost below c is distributed Poisson with parameter

$$\rho_i = \left(a_{n'} w_{n'}^{\alpha-1}\right)^{\frac{\xi}{\alpha}} \left(\sum_{\tilde{n}} a_{\tilde{n}} \bar{c}_{\tilde{n}}^{-\xi} \sum_{r \in \mathcal{R}_{\tilde{n}n'}} \prod_{k=1}^{|\mathcal{B}_r|} d_{r_{k-1},r_k}^{-\xi} \prod_{m=1}^{|\mathcal{P}_r|} \bar{t}_{p(r)_m}^{-\xi} \right) c^{\frac{\xi}{\alpha}}. \tag{30}$$

The probability that a firm i in location n (able to deliver costs below c) supplies from location n' through route r is the ratio of $\rho_{i,r}$ and ρ_i:

$$\begin{aligned}
\pi_{i,r} &= \frac{a_n c^{\frac{\xi}{\alpha}} \left(a_{n'} w_{n'}^{\alpha-1}\right)^{\frac{\xi}{\alpha}} \prod_{k=1}^{|\mathcal{B}_r|} d_{r_{k-1},r_k}^{-\xi} \prod_{m=1}^{|\mathcal{P}_r|} \bar{t}_{p(r)_m}^{-\xi} \bar{c}_n^{-\xi}}{\left(a_{n'} w_{n'}^{\alpha-1}\right)^{\frac{\xi}{\alpha}} \left(\sum_{\tilde{n}} a_{\tilde{n}} \bar{c}_{\tilde{n}}^{-\xi} \sum_{r \in \mathcal{R}_{\tilde{n}n}} \prod_{k=1}^{|\mathcal{B}_r|} d_{r_{k-1},r_k}^{-\xi} \prod_{m=1}^{|\mathcal{P}_r|} \bar{t}_{p(r)_m}^{-\xi} \right) c^{\frac{\xi}{\alpha}}} \\
&= \frac{a_n \bar{c}_n^{-\xi} \prod_{k=1}^{|\mathcal{B}_r|} d_{r_{k-1},r_k}^{-\xi} \prod_{m=1}^{|\mathcal{P}_r|} \bar{t}_{p(r)_m}^{-\xi}}{\sum_{\tilde{n}} a_{\tilde{n}} \bar{c}_{\tilde{n}}^{-\xi} \sum_{r \in \mathcal{R}_{\tilde{n}n}} \prod_{k=1}^{|\mathcal{B}_r|} d_{r_{k-1},r_k}^{-\xi} \prod_{m=1}^{|\mathcal{P}_r|} \bar{t}_{p(r)_m}^{-\xi}}
\end{aligned} \tag{31}$$

Note that the probability of sourcing from r is the same for any firm in n'. Since there are a continuum of firms in n', $\pi_{i,r}$ is also the *bilateral trade share* of route r in the total absorption of goods of destination n', denoted $\pi_{n',r}$.

Proof: Corollary 2

$$\begin{aligned}
\pi_{nn'} &= \sum_{r \in \mathcal{R}_{nn'}} \pi_{n',r} \\
&= \frac{a_n \bar{c}_n^{-\xi} \tau_{nn'}^{-\xi}}{\sum_{\tilde{n}} a_{\tilde{n}} \bar{c}_{\tilde{n}}^{-\xi} \tau_{n\tilde{n}}^{-\xi}}
\end{aligned} \tag{32}$$

where

$$\tau_{nn'} = \left(\sum_{r \in \mathcal{R}_{nn'}} \left(\prod_{k=1}^{|\mathcal{B}_r|} d_{r_{k-1},r_k}^{-\xi} \right) \left(\prod_{m=1}^{|\mathcal{P}_r|} \frac{\psi_{p(r)_m}}{\psi_{p(r)_m} + \xi} \right) \right)^{-\frac{1}{\xi}} \tag{33}$$

D.2 Closing the model

Labor market clearing: Labor demand for a firm i in location n is given by $l_i = (1 - \alpha) y_i c_i / w_n$. Plugging this condition into the labor market clearing gives:

$$L_n = \int_{i \in M_n} l_i di \Rightarrow \frac{w_n L_n}{1-\alpha} = \int_{i \in M_n} y_i c_i di. \tag{34}$$

Good market clearing:

$$y_i = L_n q_i + \sum_{n'} \int_{j \in M_{n'}} \tau_{n(j)n(j)} x_{ij} dj, \quad x_{ij} = x_j \times \mathbf{1}\{i = i^*\} \tag{35}$$

Multiplying both sides by marginal costs c_j and aggregating over firms in $M_{n'}$:

$$\underbrace{\int_{i \in M_n} c_i y_i di}_{\text{(1) Supply}} = \underbrace{L_n \int_{i \in M_n} c_i q_i di}_{\text{(2) Final good demand}} + \underbrace{\int_{i \in M_n} c_i \left[\sum_{n'} \int_{j \in M_{n'}} \tau_{n(i)n(j)} (x_j \times \mathbf{1}\{i = i^*\}) dj \right] di}_{\text{(3) Intermediate input demand}}. \tag{36}$$

Term (1) simplifies using the labor market clearing condition, $\int_{i \in M_n} c_i y_i di = w_n L_n / (1 - \alpha)$.

Term (2) simplifies as follows: With isoelastic preferences and monopolistic competition, households in city n demand $q_j = q_n p_n^{\sigma} p_j^{-\sigma}$, where $p_i = c_i \frac{\sigma}{\sigma - 1}$. Realizing that $q_n = (w_n + \Pi_n) / p_n$, where w_n is the wage rate and Π_n is the per-capita profits of firms in n rebated to labor, implies:

$$\begin{aligned}
L_n \int_{i \in M_n} c_i q_i di &= L_n (w_n + \Pi_n) p_n^{\sigma - 1} \left(\frac{\sigma}{\sigma - 1} \right)^{-\sigma} \int_{i \in M_n} c_i^{1-\sigma} di \\
&= L_n (w_n + \Pi_n) \left(\left(\int_{i \in M_n} p_i^{1-\sigma} di \right)^{\frac{1}{1-\sigma}} \right)^{\sigma - 1} \left(\frac{\sigma}{\sigma - 1} \right)^{-\sigma} \int_{i \in M_n} c_i^{1-\sigma} di \\
&= L_n (w_n + \Pi_n) \left(\frac{\sigma}{\sigma - 1} \right)^{-1} \left(\int_{i \in M_n} c_i^{1-\sigma} di \right)^{-1} \int_{i \in M_n} c_i^{1-\sigma} di \\
&= L_n (w_n + \Pi_n) \tilde{\sigma}^{-1}.
\end{aligned} \tag{37}$$

[Note: term (2) simplifies also easily when considering that $q_n p_n = \int_{i \in M_n} \tilde{\sigma} c_i q_i di$, where $\tilde{\sigma} = \sigma / (\sigma - 1)$, and $q_n p_n = w_n + \Pi_n$.] It remains to characterize per-capita profit rebated to households in city n. Note that firms only gain profits from selling final goods to local households:

$$\text{Profit}_i = p_i q_i L_n - c_i q_i L_n. \tag{38}$$

Therefore, total profit per capita (aggregating over all firms in M_n) yields:

$$\begin{aligned}\Pi_n &= L_n^{-1}\int_{i\in M_n} L_n(p_i q_i - c_i q_i)di \\ &= \int_{i\in M_n}(\tilde{\sigma}c_i q_i - c_i q_i)di \\ &= (\tilde{\sigma}-1)\int_{i\in M_n} c_i q_i di \\ &= (\tilde{\sigma}-1)\tilde{\sigma}^{-1}q_n p_n \\ &= \frac{1}{\sigma}(w_n+\Pi_n).\end{aligned}\tag{39}$$

Solving for per-capita profits yields $\Pi_n = \frac{w_n}{\sigma-1}$. Therefore, term (2) simplifies to:

$$\begin{aligned}L_n\int_{i\in M_n} c_i q_i di &= L_n\left(w_n + \frac{w_n}{\sigma-1}\right)\tilde{\sigma}^{-1} \\ &= L_n w_n.\end{aligned}\tag{40}$$

Term (3) simplifies as follows: Firms demand $x_j = \frac{(1-\alpha)y_j c_j}{c_i \tau_{n(i)n(j)}}$ units of intermediate inputs. This implies:

$$\begin{aligned}\int_{i\in M_n} c_i\left(\sum_{n'}\int_{j\in M_{n'}}\tau_{nn'}(x_j\times \mathbf{1}\{i=i^*\})dj\right)di &= \alpha\int_{i\in M_n}\left(\sum_{n'}\int_{j\in M_{n'}}\mathbf{1}\{i=i^*\}y_j c_j dj\right)di \\ &= \alpha\sum_{n'}\int_{j\in M_{n'}}\mathbf{1}\{i^*\in M_n\}y_j c_j dj \\ &= \alpha\sum_{n'}\pi_{nn'}\int_{j\in M_{n'}} y_j c_j dj \\ &= \alpha\sum_{n'}\pi_{nn'}\frac{w_{n'}L_{n'}}{1-\alpha}\end{aligned}\tag{41}$$

Putting terms (1), (2) and (3) together yields the following system for city-level wages:

$$w_n L_n = \sum_{n'}\pi_{nn'}w_{n'}L_{n'}.\tag{42}$$

Note that, if the technological constant α is city-specific, the system reads:

$$\frac{\alpha_n}{1-\alpha_n}w_n L_n = \sum_{n'}\frac{\alpha_{n'}}{1-\alpha_{n'}}\pi_{nn'}w_{n'}L_{n'}.\tag{43}$$

Finally, to obtain traffic, we recover the value of bilateral flows (i.e. the level of expenditures from firms in n' to firms in n):

$$
\begin{aligned}
X_{nn'} &= \int_{i\in M_n}\int_{j\in M_{n'}} c_i\tau_{nn'}(x_j \times \mathbf{1}\{i=i^*\})djdi \\
&= \alpha \int_{i\in M_n}\int_{j\in M_{n'}} \mathbf{1}\{i=i^*\} y_j c_j djdi \\
&= \alpha \int_{j\in M_{n'}} \mathbf{1}\{i^* \in M_n\} y_j c_j dj \\
&= \alpha \pi_{nn'} \int_{j\in M_{n'}} y_j c_j dj \\
&= \alpha \pi_{nn'} \frac{w_{n'}L_{n'}}{1-\alpha}
\end{aligned}
\tag{44}
$$

D.3 General equilibrium: definition

Given a geography $\mathcal{G} = \{\mathcal{N},\mathcal{P},\mathcal{L},\mathcal{M},\mathcal{A},\mathcal{D},\mathcal{K}_p\}$ and a vector of model parameters $\{\alpha,\xi,\lambda_1,\lambda_2,\lambda_3,\{\psi_p\}_{p\in\mathcal{P}}\}$, an equilibrium is defined as a distribution of wages and factory-gate prices $\{w_n,\bar{c}_n\}_{n\in\mathcal{N}}$, such that:

1. Given the equilibrium transportation network $\delta_{ll'} \in \{\delta_{ll'}\}_{l,l'\in\mathcal{N}\cup\mathcal{P}\times\mathcal{N}\cup\mathcal{P}}$, (i) consumers maximize utility; (ii) firms choose the techniques and the routes that minimize costs, and markups that maximize profits; and (iii) market clears.[38]

2. Given the transportation network fundamentals $\{\mathcal{D},\mathcal{K}_p\}$ an equilibrium prices, the equilibrium transportation network $\delta_{ll'} \in \{\delta_{ll'}\}_{l,l'\in\mathcal{N}\cup\mathcal{P}\times\mathcal{N}\cup\mathcal{P}}$ is determined by the equilibrium levels of traffic $\{\Xi_p\}$.

This leads the equilibrium to be characterized by the following set of equations:[39]

$$w_nL_n = \frac{1-\alpha}{\alpha}\sum_{n'} X_{nn'} \quad (\textit{wage bill})$$

$$\pi_{nn'} = \frac{a_n\bar{c}_n^{-\xi}\tau_{nn'}^{-\xi}}{\sum_{\tilde{n}} a_{\tilde{n}}\bar{c}_{\tilde{n}}^{-\xi}\tau_{\tilde{n}n'}^{-\xi}} \quad (\textit{bilateral trade shares})$$

$$\bar{c}_n^{-\xi} = a_n^{\xi} w_n^{(\alpha-1)\xi}\left(\sum_{\tilde{n}} a_{\tilde{n}}\bar{c}_{\tilde{n}}^{-\xi}\tau_{\tilde{n}n}\right)^{\alpha}\Gamma(1-\alpha) \quad (\textit{factory-gate cost indices})$$

$$[\tau_{nn'}] = \begin{cases} 1 & \text{if} \quad n=n' \\ \left[(I-\Delta)^{-1}\right]^{\circ\left(-\frac{1}{\xi}\right)} & \text{otherwise} \end{cases} \quad (\textit{transportation costs})$$

[38]Formally, the economy admits ports as cities. However, I assume that ports have a 0 measure of households and firms, such that they do not consume or produce. It results that equilibrium prices have dimension $|\mathcal{N}|$, while the transportation network has dimensions $(|\mathcal{N}\cup\mathcal{P}|)^2$.

[39]Up to a numeraire: $w_1 = 1$.

$$\Delta = [\delta_{ll'}], \quad \delta_{ij} = \begin{cases} d_{ll'}^{-\xi} \bar{t}_{l'}^{-\xi} & \text{if} \quad l' \in \mathcal{P} \\ d_{ll'}^{-\xi} & \text{otherwise} \end{cases} \qquad (\textit{transportation network})$$

$$d_{ll'}^{-\xi} = \epsilon_{ll'}^{\lambda_1}, \quad \bar{t}_{l'}^{-\xi} = \Xi_{l'}^{\lambda_2} K_{l'}^{\lambda_3} \frac{\psi_{l'}}{\psi_{l'} + \xi} \quad (\textit{link- and port-level costs})$$

$$\Xi_p = \delta_{pp} \sum_n \sum_{n'} \left(\tau_{np} \tau_{pn'} \tau_{nn'}^{-1} \right)^{-\xi} X_{nn'} \quad (\textit{link- and port-level traffic})$$

$$X_{nn'} = \alpha \pi_{nn'} \frac{w_{n'} L_{n'}}{1-\alpha} \quad (\textit{bilateral trade})$$

D.4 General equilibrium: numerical algorithm

Given a set of geography fundamentals $\mathcal{G} = \{\mathcal{N}, \mathcal{P}, \mathcal{L}, \mathcal{M}, \mathcal{A}, \mathcal{D}, \mathcal{K}_p\}$ and a set of model parameters $\{\sigma, \alpha, \xi, \lambda_1, \lambda_2, \lambda_3, \{\psi_p\}_{p \in \mathcal{P}}\}$, the following algorithm solves for the equilibrium of the economy:

1. **Initialize** endogenous variables:
   (a) $\{w_n\}_{n \in \mathcal{N}}$ (wages)
   (b) $\{\bar{c}_n\}_{n \in \mathcal{N}}$ (factory-gate cost indices)
   (c) $\{\pi_{nn'}\}_{n,n' \in \mathcal{N}^2}$ (bilateral trade shares)
   (d) $\{\Xi_p\}_{p \in \mathcal{P}}$ (port traffic)
2. **Outer-loop** — While $distance_{wages} > tol$ or $distance_{traffic} > tol$:
   (a) Based on distances $\epsilon_{ll'}$, port capacity K_p and traffic Ξ_p, update Λ (*transportation network*)
   (b) Based on Λ, update transportation costs $\tau_{ll'}$ (*transportation costs*)
   (c) **Inner-loop (factory-gate costs)** — While $distance_{costs} > tol$:
      i. Based on transportation costs $\tau_{nn'}$, city-level productivity a_n, factory-gate costs indices $\bar{c}_n$, and wages w_n, update $\bar{c}_n$ (*factory-cost indices*)[40]
      ii. Compute $distance_{costs} = \sum_n \left[(\bar{c}_n)^{i_c} - (\bar{c}_n)^{i_c+1} \right]^2$, with i_c = iteration (inner-loop)
   (d) Based on transportation costs $\tau_{nn'}$, city-level productivity a_n, factory-gate costs indices $\bar{c}_n$, and wages w_n, update $\pi_{nn'}$ (*bilateral trade shares*)
   (e) Based on bilateral trade shares $\pi_{nn'}$ and wages bills $w_n L_n$, update $X_{nn'}$ (*bilateral trade*)

[40]Note that transportation costs used in factory-gate cost indices and bilateral trade shares do not have the same dimension as transportation costs used for traffic. This is because ports have a measure 0 of firms, and therefore would not impact bilateral trade shares and costs indices. I use only the sub-matrix of τ_{ij} with dimensions $|N| \times |N|$.

(f) Based on the transportation network Λ and bilateral trade $X_{nn'}$, compute Ξ_p (*port-level traffic*)

(g) Based on bilateral trade $X_{nn'}$, and households L_n compute wages w_n (*wage bills*), up to a normalization $w_1 = 1$

(h) Compute $distance_{wages} = \sum_n \left[(w_n)^{i_{\text{out}}} - (w_n)^{i_{\text{out}}+1}\right]^2$ and $distance_{traffic} = \sum_p \left[(\Xi_p)^{i_{\text{out}}} - (\Xi_p)^{i_{\text{out}}+1}\right]^2$, with $i_{\text{out}} =$ iteration (outer loop)

D.5 Welfare

Define welfare in location d as:

$$\begin{aligned} V_n &= \frac{L_n(w_n + \Pi_n)}{\left(\int_{i\in M_n} p_i^{1-\sigma} di\right)^{\frac{1}{1-\sigma}}} \\ &= \frac{L_n w_n \tilde{\sigma}}{\left(\int_{i\in M_n} (\tilde{\sigma} c_i)^{1-\sigma} di\right)^{\frac{1}{1-\sigma}}} \\ &= \frac{L_n w_n}{\left(M_n \int c^{1-\sigma} dF_i(c)\right)^{\frac{1}{1-\sigma}}} \end{aligned} \tag{45}$$

It remains to characterize $\int c^{1-\sigma} dF_i(c)$:

$$\begin{aligned} \int c^{1-\sigma} dF_i(c) &= \int_0^\infty c^{1-\sigma} d\left\{1 - exp\left[-\left(a_n w_n^{\alpha-1}\right)^{\frac{\xi}{\alpha}} \left(\sum_{n'} a_{n'} \bar{c}_{n'}^{-\xi} \sum_{r\in\mathcal{R}_{n'n}} \prod_{k=1}^{|\mathcal{B}_r|} d_{r_{k-1},r_k}^{-\xi} \prod_{m=1}^{|\mathcal{P}_r|} \bar{t}_{p(r)_m}^{-\xi}\right) c^{\frac{\xi}{\alpha}}\right]\right\} \\ &= \int_0^\infty c^{1-\sigma} d\left\{1 - exp\left[-\left(a_n w_n^{\alpha-1}\right)^{\frac{\xi}{\alpha}} \left(\sum_{n'} a_{n'} \bar{c}_{n'}^{-\xi} \tau_{n'n}\right) c^{\frac{\xi}{\alpha}}\right]\right\} \\ &= \left[a_n w_n^{\alpha-1} \left(\sum_{n'} a_{n'} \bar{c}_{n'}^{-\xi} \tau_{n'n}\right)^{\frac{\alpha}{\xi}}\right]^{\sigma-1} \int_0^\infty u^{1-\sigma} d\left\{1 - exp\left[-u^{\frac{\xi}{\alpha}}\right]\right\} \\ &= \left[a_n w_n^{\alpha-1} \left(\sum_{n'} a_{n'} \bar{c}_{n'}^{-\xi} \tau_{n'n}\right)^{\frac{\alpha}{\xi}}\right]^{\sigma-1} \int_0^\infty v^{-\frac{\alpha(\sigma-1)}{\xi}} d\left\{1 - e^{-v}\right\} \\ &= \left[a_n w_n^{\alpha-1} \left(\sum_{n'} a_{n'} \bar{c}_{n'}^{-\xi} \tau_{n'n}\right)^{\frac{\alpha}{\xi}}\right]^{\sigma-1} \int_0^\infty v^{-\frac{\alpha(\sigma-1)}{\xi}} e^{-v} dv \\ &= \left[a_n w_n^{\alpha-1} \left(\sum_{n'} a_{n'} \bar{c}_{n'}^{-\xi} \tau_{n'n}\right)^{\frac{\alpha}{\xi}}\right]^{\sigma-1} \Gamma\left(1 - \frac{\alpha(\sigma-1)}{\xi}\right), \end{aligned} \tag{46}$$

The third equality follows from applying the transformation $a_n w_n^{\alpha-1} \left(\sum_{n'} a_{n'} \bar{c}_{n'}^{-\xi} \tau_{n'n}\right)^{\frac{\alpha}{\xi}} c = u$. The fourth equality follows from applying the transformation $v = u^{\frac{\xi}{\alpha}}$. The sixth equality follows from the definition of the Gamma function $\Gamma(z) = \int_0^\infty t^{z-1}e^{-t}dt$. Therefore, welfare writes:

$$V_n = L_n w_n M_n^{\frac{1}{\sigma-1}} \left[a_n w_n^{\alpha-1} \left(\sum_{n'} a_{n'} \bar{c}_{n'}^{-\xi} \tau_{n'n} \right)^{\frac{\alpha}{\xi}} \right]^{\sigma-1} \Gamma\left(1 - \frac{\alpha(\sigma-1)}{\xi}\right) \tag{47}$$